CASE FILE
COPY

NACA RM L56L19

NACA

RESEARCH MEMORANDUM

LONGITUDINAL AND LATERAL STABILITY AND CONTROL CHARACTERISTICS OF TWO CANARD AIRPLANE CONFIGURATIONS AT MACH NUMBERS OF 1.41 AND 2.01

By Cornelius Driver

Langley Aeronautical Laboratory
Langley Field, Va.

NATIONAL ADVISORY COMMITTEE
FOR AERONAUTICS

WASHINGTON

April 10, 1957
Declassified October 28, 1960

NATIONAL ADVISORY COMMITTEE FOR AERONAUTICS

RESEARCH MEMORANDUM

LONGITUDINAL AND LATERAL STABILITY AND CONTROL CHARACTERISTICS OF TWO CANARD AIRPLANE CONFIGURATIONS AT MACH NUMBERS OF 1.41 AND 2.01

By Cornelius Driver

SUMMARY

An investigation has been conducted in the Langley 4- by 4-foot supersonic pressure tunnel to determine the aerodynamic characteristics in pitch and sideslip of a canard airplane model at Mach numbers of 1.41 and 2.01. The body of the model had a fineness ratio of 10.57 and was equipped with a trapezoidal canard surface with an area 12 percent of the wing area. Two wings of equal area but differing in plan form were investigated. One had a trapezoidal plan form with an unswept 80-percent-chord line, an aspect ratio of 3, and a taper ratio of 0.143; the other had a 60° delta plan form with an aspect ratio of 2.31. The model was equipped with a low-aspect-ratio vertical tail and twin ventral fins.

The canards were highly effective in producing pitching moments which resulted in large increments of trim lift coefficient with small control deflections and no decrease in lift-curve slope, so that relatively high values of trim lift coefficient and trim lift-drag ratios were obtained. The delta-wing configuration had a maximum trimmed lift-drag ratio of 4.8 at a Mach number of 1.41 and 5.0 at a Mach number of 2.01. Both the presence of the canard and deflections of the canard caused a reduction in the directional stability, particularly at high angles of attack. However, the delta-wing configuration maintained directional stability up to angles of attack of 12.5° at a Mach number of 2.01. The effective dihedral was positive throughout the angle-of-attack and Mach number ranges investigated. Canard deflection caused a substantial increase in the positive effective dihedral.

INTRODUCTION

Conventional aircraft in advancing from subsonic to supersonic flight generally experience an increase in longitudinal stability. This increase in longitudinal stability results from a rearward shift in the wing center of pressure as well as from wing-lift carryover to the fuselage afterbody and the loss of wing downwash at the horizontal tail. Because of the increased longitudinal stability at supersonic speeds large deflections of the horizontal tail are required for trimming, with an attendant loss in lift, increase in drag, and decrease in maneuvering capability.

One approach for alleviating the stability increase is through the use of a delta-wing tailless configuration whereby the center-of-pressure shift is minimized and the downwash changes at the tail and the wing-lift carryover effects are eliminated. However, for the tailless configuration the deflection of a trailing-edge flap for control results in a decrease in total lift as well as an increase in drag. These conditions are generally further aggravated by the large deflection angles required because of the inherently short moment arms for such controls. In addition, little excess control deflection may be available to provide for maneuvering.

Logically, another approach to consider would be the use of a canard arrangement which removes the control from the region of wing downwash and minimizes the wing-lift carryover effects by virtue of the short fuselage afterbodies usually employed. The control effectiveness of the canard would be maintained as high as possible through the use of a long moment arm with only small deflections and lifts required so that the wake effects and drag from the canard would be minimized. The use of a long moment arm is compatible with the need for high-fineness-ratio bodies at supersonic speeds but may be restricted by the nonlinear moment characteristics of long bodies. The adverse effects of the long body on the directional characteristics of the canard configuration would be as severe as for conventional configurations. In addition, the wake effects from the forward surface may further affect the directional characteristics.

In the past, the canard configurations have encountered serious subsonic problems. These problems have been primarily that of providing longitudinal trim at maximum lift (ref. 1), adverse directional effects at high lifts (ref. 2), and limited center-of-gravity travel (ref. 3). It would be expected that some of these subsonic problems may still be present, but the performance and trim-lift benefits possible at supersonic speeds prompts renewed effort in solving these subsonic difficulties.

In view of the supersonic performance gains to be expected from canard configurations, a research program has been initiated at the Langley 4- by 4-foot supersonic pressure tunnel to determine the aerodynamic characteristics of a generalized canard airplane configuration at supersonic speeds. Although provisions were made for testing the complete model and various combinations of its component parts, only data for the complete model and canard-off configurations are presented in the present report.

This paper presents the static longitudinal and lateral stability and control results obtained at Mach numbers of 1.41 and 2.01 for two complete model configurations. The two configurations differed only in wing plan form. One wing had a trapezoidal plan form with an unswept 80-percent-chord line, an aspect ratio of 3, and a taper ratio of 0.143. The other wing had a 60° delta plan form with an aspect ratio of 2.31. The two wings had equal areas. A trapezoidal canard surface having a total area 12 percent of the wing area was used for both configurations. The configurations were equipped with a low-aspect-ratio swept vertical tail and twin ventral fins. The models were tested at angles of attack to about 25° with canard deflections of 0°, 5°, 10°, and 15°. Sideslip tests were made to angles of sideslip of about 24° at angles of attack from 0° to 24° and with canard deflections of 0° and 15°.

SYMBOLS

The results are presented as force and moment coefficients with lift, drag, and pitching moment referred to the stability axis system and rolling moment, yawing moment, and side force referred to the body axis system (fig. 1). The reference center of moments was at body station 25 which corresponds to a location 17.8 percent $\bar{c}$ ahead of the leading edge of the wing mean geometric chord for the trapezoidal wing and to a point 7.75 percent $\bar{c}$ behind the leading edge of the wing mean geometric chord for the delta wing.

C_L lift coefficient, $\frac{F_L}{qS}$

C_D' approximate drag coefficient equal to C_D at zero sideslip, $\frac{F_D'}{qS}$

C_m pitching-moment coefficient, $\frac{M_{Ys}}{qS\bar{c}}$

C_l rolling-moment coefficient, $\frac{M_X}{qSb}$

C_n yawing-moment coefficient, $\frac{M_Z}{qSb}$

C_Y side-force coefficient, $\frac{F_Y}{qS}$

F_L lift force

F'_D drag force

M_Y moment about Y-axis

M_X moment about X-axis

M_Z moment about Z-axis

F_Y side force

q free-stream dynamic pressure

S wing area including fuselage intercept

b span

$\bar{c}$ wing mean geometric chord (M.G.C.)

h altitude, ft

M free-stream Mach number

α angle of attack of fuselage reference line, deg

β angle of sideslip of fuselage reference line, deg

δ_c deflection angle of canard with respect to fuselage reference line, positive when trailing edge is down, deg

C_{n_β} directional-stability parameter, $\frac{\partial C_n}{\partial \beta}$

C_{l_β} effective-dihedral parameter, $\frac{\partial C_l}{\partial \beta}$

C_{Y_β} side-force parameter, $\frac{\partial C_Y}{\partial \beta}$

Subscript:

s denotes stability-axis system

MODELS AND APPARATUS

Details of the model are shown in figures 2 and 3 and the geometric characteristics are presented in table I.

The body of the model was composed of a parabolic nose followed by the frustum of a cone which was faired into a cylinder. The resultant body fineness ratio was 10.57. Coordinates of the body are given in table II. Details of the trapezoidal canard surface are also shown in figure 2. The ratio of the total canard area to total wing area was 0.115. The canard surface was motor driven and deflections were set by remote control. Details of the delta and trapezoidal wings are shown in figure 2(b). The wings had hexagonal sections and aspect ratios of 2.31 and 3.00, respectively.

Force measurements were made through the use of a six-component internal strain-gage balance. The model was mounted in the tunnel on a remote-controlled rotary sting. The sting-angle range was varied from 0° to about 25° at various roll angles from 0° to 90°.

TESTS, CORRECTIONS, AND ACCURACY

The test conditions are summarized in the following table:

	M = 1.41	M = 2.01
Stagnation temperature, °F	100	100
Stagnation pressure, lb/sq ft abs	1,440	1,440
Reynolds number based on $\bar{c}$ of delta wing	3.24×10^6	2.68×10^6
Reynolds number based on $\bar{c}$ of trapezoidal wing	2.54×10^6	2.10×10^6

The stagnation dewpoint was maintained sufficiently low (-25° F or less) so that no condensation effects were encountered in the test section.

The angles of attack and sideslip were corrected for the deflection of the balance and sting under load. The Mach number variation in the test section was approximately ±0.01 and the flow-angle variation in the vertical and horizontal planes did not exceed about ±0.1°. No corrections were considered necessary to correct for these flow variations. The base pressure was measured and the drag was adjusted to a base pressure equal to free-stream static pressure.

The estimated repeatability of the individual measured quantities are as follows:

C_L	±0.0003
C_D	±0.001
C_m	±0.0004
C_l	±0.0004
C_n	±0.0001
C_Y	±0.0015
α, deg	±0.2
β, deg	±0.2
δ_c, deg	±0.1

PRESENTATION OF RESULTS

The basic results presenting the aerodynamic characteristics in pitch are presented in figures 4 to 7. The basic lateral results are shown in figures 8 to 11.

A summary of the longitudinal trim characteristics are presented in figures 12, 13, and 14. The sideslip derivatives are summarized in figure 15.

DISCUSSION

Longitudinal Characteristics

A significant characteristic of the canard configuration is the fact that the canard control when deflected for trimming has essentially no effect on the total lift (figs. 4 to 7). This is in contrast to conventional tail-rearward configurations wherein the tail deflections required for trimming produce substantial reductions in lift. (See refs. 4 and 5, for example.) Hence, when trimming with conventional tail-rearward configurations, it is necessary to increase the angle of

attack in order to maintain a constant lift whereas with the canard configuration the deflection of the control for trimming requires essentially no change in the angle of attack. The increase in angle of attack required in trimming conventional configurations causes an added increment of drag that does not arise for the canard configuration.

The canard control offers other advantages in that small deflections of the canard may be highly effective in providing moments which result in higher trim lift coefficients because of the long moment arm available and because the lift required to trim is positive. The advantages of high trim lift coefficients at small control deflections and small angles of attack are apparent in the trimmed lift-drag ratios wherein relatively high values of L/D are obtained at low lift coefficients. The delta-wing configuration, for example, had a maximum trimmed lift-drag ratio of 4.8 at $M = 1.41$ and 5.0 at $M = 2.01$ (fig. 12). It is significant that the lift-drag ratios are high in the lower lift range since this is the range of lift coefficient required for level flight at high altitudes and supersonic speeds. For example if the delta-wing configuration had a wing loading of 90 lb/sq ft at $M = 2.01$, then the maximum trim lift coefficient available for a canard deflection of 15° would permit level flight at 61,000 feet. (See fig. 14.)

It should be recognized that the absolute values of L/D would be subject to detail model differences and would be lowered if air inlets and a canopy were added to the model. However, the significant trim advantages noted for the canard configurations in comparison with conventional configurations should still be realized.

Compared on the basis of the same center of moments (body station 25), the delta-wing configuration exhibited slightly better longitudinal trim characteristics (fig. 12) since this arrangement had the lower static margin. When the static margin for the trapezoidal wing is reduced to that for the delta wing (22 percent $\bar{c}$), the trapezoidal-wing configuration could be trimmed to higher maximum values of L/D (fig. 13). Since the pitching-moment results obtained for both configurations indicate a reasonably linear variation with lift coefficient through a large lift range, it would be possible to reduce the static margin through a rearward shift of the center of gravity so that additional increases in trim lift-drag ratio and in trim lift coefficient might be obtained. For example, for the delta-wing configuration at $M = 2.01$, it was found that by decreasing the static margin from 22 percent to 15 percent of the mean geometric chord the maximum trim lift-drag ratio was increased from 5.0 to 5.6 and the maximum trim lift coefficient from 0.237 to 0.385. However, the extent to which the center of gravity can be moved rearward to further the supersonic performance gains depends upon the static margin at subsonic speeds as well as the center-of-gravity location for which neutral directional stability would occur.

Lateral Characteristics

The directional stability characteristics of the canard configurations (fig. 15) are similar to those for other current aircraft types insofar as the reduction in C_{n_β} with increasing angle of attack is concerned (ref. 6). This similarity might be expected because of the short moment arm of the vertical tail. For both wing configurations, either the presence of the canard surface or canard deflection caused a reduction in the directional stability, particularly at the higher angles of attack (figs. 8 to 11). Positive directional stability was maintained, however, to $\alpha = 12.5^\circ$ for the delta-wing configuration at $M = 2.01$ (fig. 15(b)). The directional stability characteristics at angle of attack could be improved at these Mach numbers by the use of a higher-aspect-ratio vertical tail or a ventral fin with more area rearward of the center of gravity.

Positive effective dihedral (negative C_{l_β}) was indicated throughout the angle-of-attack and Mach number ranges investigated (fig. 15). The presence of the canards provided a negative C_{l_β} increment that was evident up to $\alpha \approx 14^\circ$ at $M = 2.01$. Above $\alpha \approx 14^\circ$, the presence of the canard (for the delta-wing configuration) indicated a positive increment of C_{l_β}. Canard deflections caused a further increase in the positive effective dihedral (figs. 9 and 11).

The presence of the canard provided decreases in C_{Y_β} at high angles of attack (8° to 16°) that were generally consistent with the decreases in C_{n_β}.

CONCLUSIONS

An investigation has been made in the Langley 4- by 4-foot supersonic pressure tunnel at Mach numbers of 1.41 and 2.01 to determine the longitudinal and lateral stability characteristics of a generalized canard airplane configuration equipped either with a delta-plan-form wing or with a trapezoidal-plan-form wing. The results of the investigation indicate the following conclusions:

1. The canards were highly effective in producing pitching moments which resulted in large increments of trim lift coefficient with small control deflections and no decrease in lift-curve slope, so that relatively high values of trim lift coefficient and trim lift-drag ratios

were obtained. The delta-wing configuration had a maximum trimmed lift-drag ratio of 4.8 at a Mach number of 1.41 and 5.0 at a Mach number of 2.01.

2. For each wing configuration, both the presence of the canard and deflections of the canard caused a reduction in directional stability C_{n_β}, particularly at high angles of attack. However, the delta-wing configuration maintained directional stability up to angles of attack of 12.5° at a Mach number of 2.01.

3. Positive effective dihedral (negative C_{l_β}) was indicated throughout the angle-of-attack and Mach number ranges investigated. Canard deflection provided a substantial increase in the positive effective dihedral.

Langley Aeronautical Laboratory,
National Advisory Committee for Aeronautics,
Langley Field, Va., December 3, 1956.

REFERENCES

1. Mathews, Charles W.: Study of the Canard Configuration With Particular Reference to Transonic Flight Characteristics and Low-Speed Characteristics at High Lift. NACA RM L8G14, 1949.

2. Johnson, Joseph L., Jr., and Paulson, John W.: Free-Flight-Tunnel Investigation of the Low-Speed Stability and Control Characteristics of a Canard Airplane Model. NACA RM L53I11, 1953.

3. Bates, William R.: Low-Speed Static Longitudinal Stability Characteristics of a Canard Model Having a 60° Triangular Wing and Horizontal Tail. NACA RM L9H17, 1949.

4. Palazzo, Edward B., and Sprearman, M. Leroy: Static Longitudinal and Lateral Stability and Control Characteristics of a Model of a 35° Swept-Wing Airplane at a Mach Number of 1.41. NACA RM L54G08, 1955.

5. Spearman, M. Leroy, Driver, Cornelius, and Robinson, Ross B.: Aerodynamic Characteristics of Various Configurations of a Model of a 45° Swept-Wing Airplane at a Mach Number of 2.01. NACA RM L54J08, 1955.

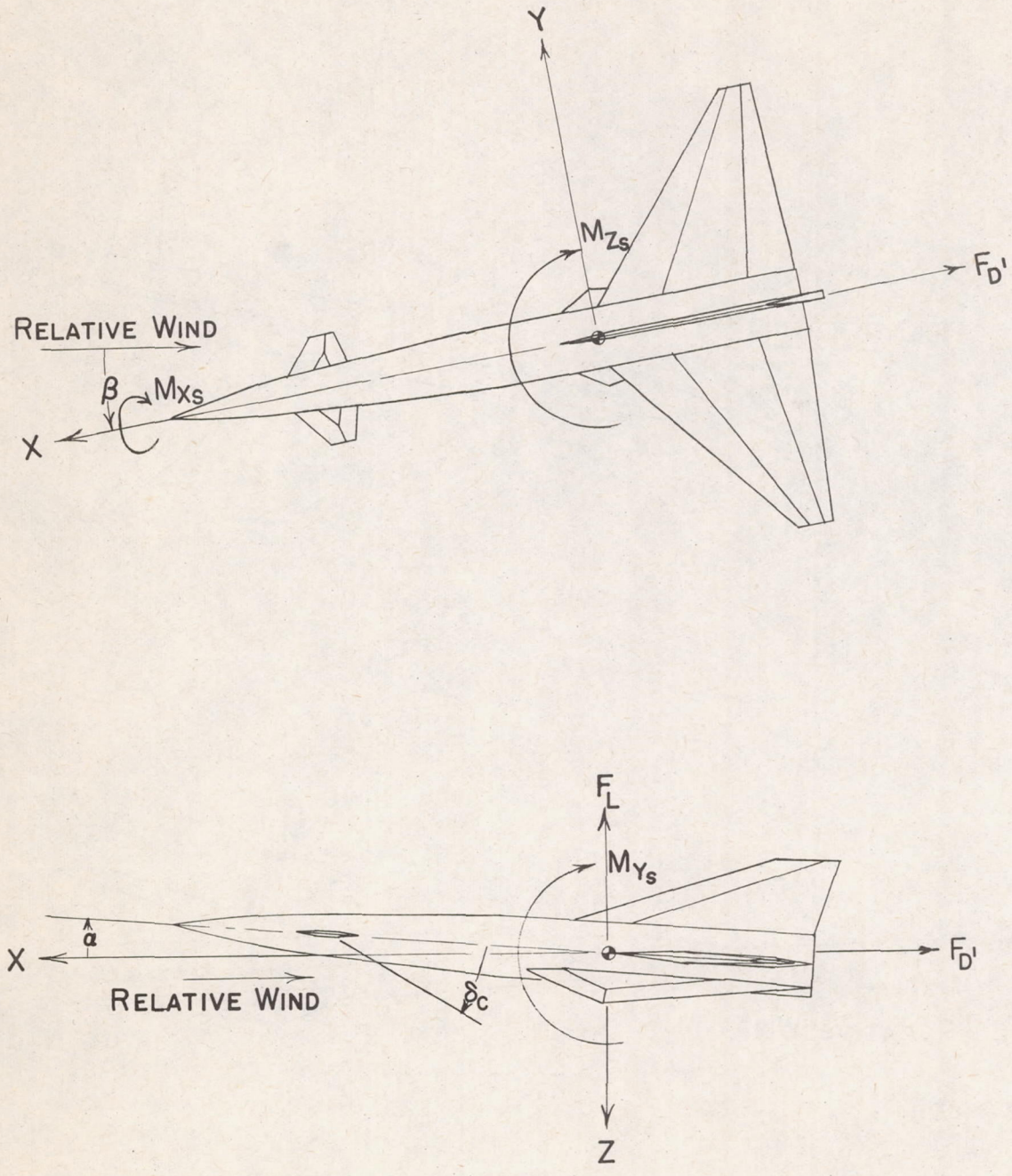
6. Spearman, M. Leroy, and Robinson, Ross B.: Static Lateral Stability and Control Characteristics of a Model of a 45° Swept-Wing Fighter Airplane With Various Vertical Tails at Mach Numbers of 1.41, 1.61, and 2.01. NACA RM L56D05, 1956.

TABLE I.- GEOMETRIC CHARACTERISTICS OF MODEL

Body:	
Maximum diameter, in.	3.50
Length, in.	37.00
Base area, sq in.	9.582
Fineness ratio	10.57
Trapezoidal wing:	
Span, in.	25.72
Chord at body-wing intersection, in.	13.25
Area, sq ft	1.53
Aspect ratio	3
Taper ratio	0.143
Thickness ratio	0.04
Mean geometric chord, in.	10.184
Sweep angle of leading edge	$38^{\circ}40'$
Sweep angle of trailing edge	$-11^{\circ}-18'$
Leading-edge half-angle, normal to L.E., deg	5
Trailing-edge half-angle, normal to T.E., deg	5
Delta wing:	
Span, in.	22.56
Chord at body wing intersection, in.	16.51
Mean geometric chord, in.	13.027
Area, sq ft	1.53
Aspect ratio	2.31
Thickness ratio	0.036
Leading-edge half-angle, normal to L.E., deg	5
Trailing-edge half-angle, normal to T.E., deg	5
Canard:	
Area (total to body center line), sq in.	25.354
Area, exposed (each canard), sq in.	6.742
Span, exposed, in.	2.25
Mean geometric chord, in.	3.33
Ratio of total canard area to total wing area	0.115
Vertical tail:	
Area, exposed, sq ft	0.279
Span, exposed, in.	4.25
Aspect ratio	0.439
Sweep of leading edge, deg	70
Section	3/16 in. slab
Leading-edge half-angle, normal to L.E., deg	5
Ventral fins:	
Area, each fin, exposed, sq ft	0.13
Span, exposed, in.	2.25
Aspect ratio	0.271
Sweep of leading edge, deg	60
Sweep of trailing edge, deg	-77.5
Leading-edge half-angle, normal to L.E., deg	5
Trailing-edge half-angle, normal to T.E., deg	5

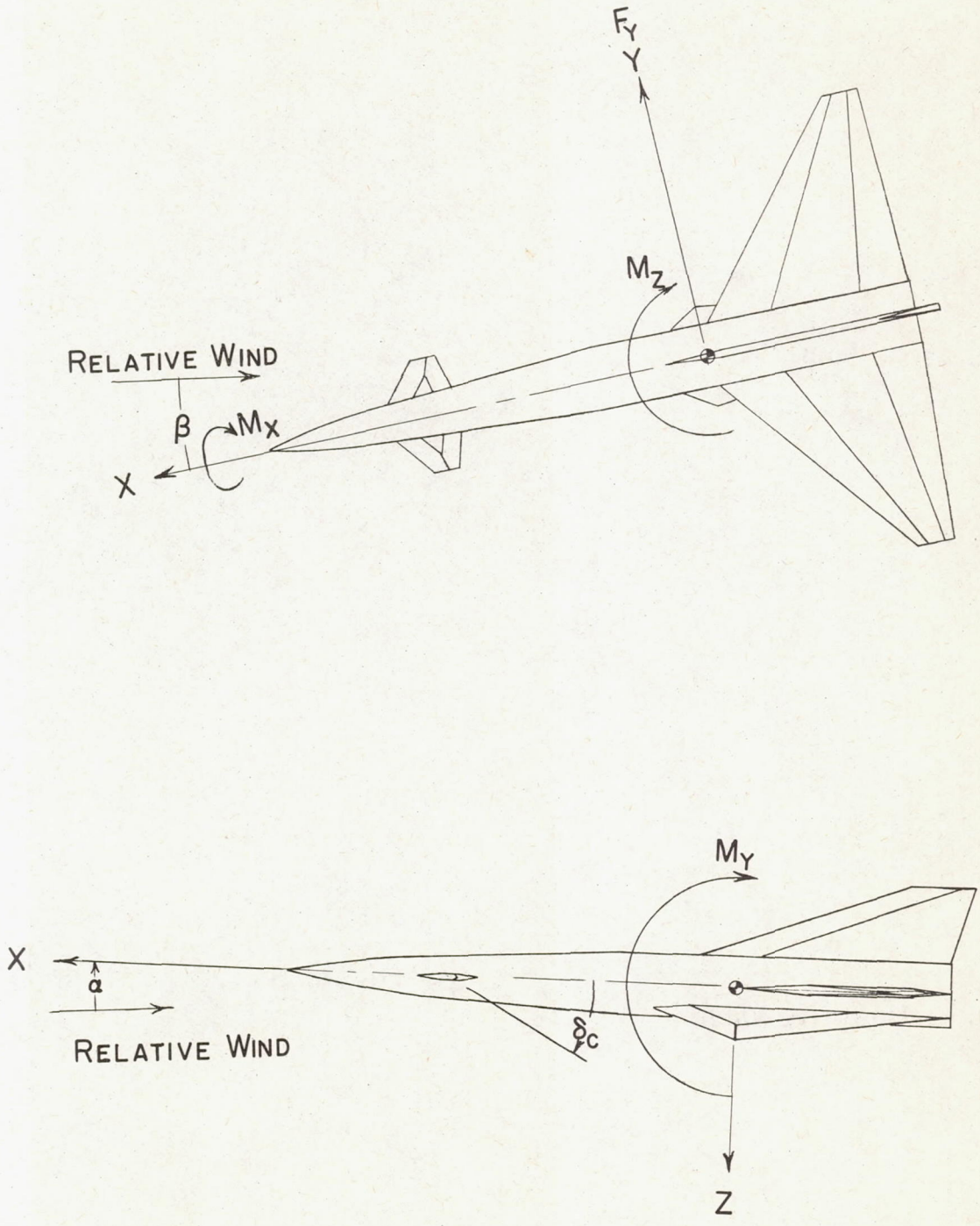
TABLE II.- COORDINATES OF BODY

Body station	Radius	
0	0	
.297	.076	
.627	.156	
.956	.233	
1.285	.307	
1.615	.378	
1.945	.445	
2.275	.509	
2.605	.573	
2.936	.627	
3.267	.682	
3.598	.732	
3.929	.780	
4.260	.824	
4.592	.865	
4.923	.903	
5.255	.940	
5.587	.968	
5.920	.996	
6.252	1.020	
6.583	1.042	Conical section
18.648	1.75	
37.000	1.75	



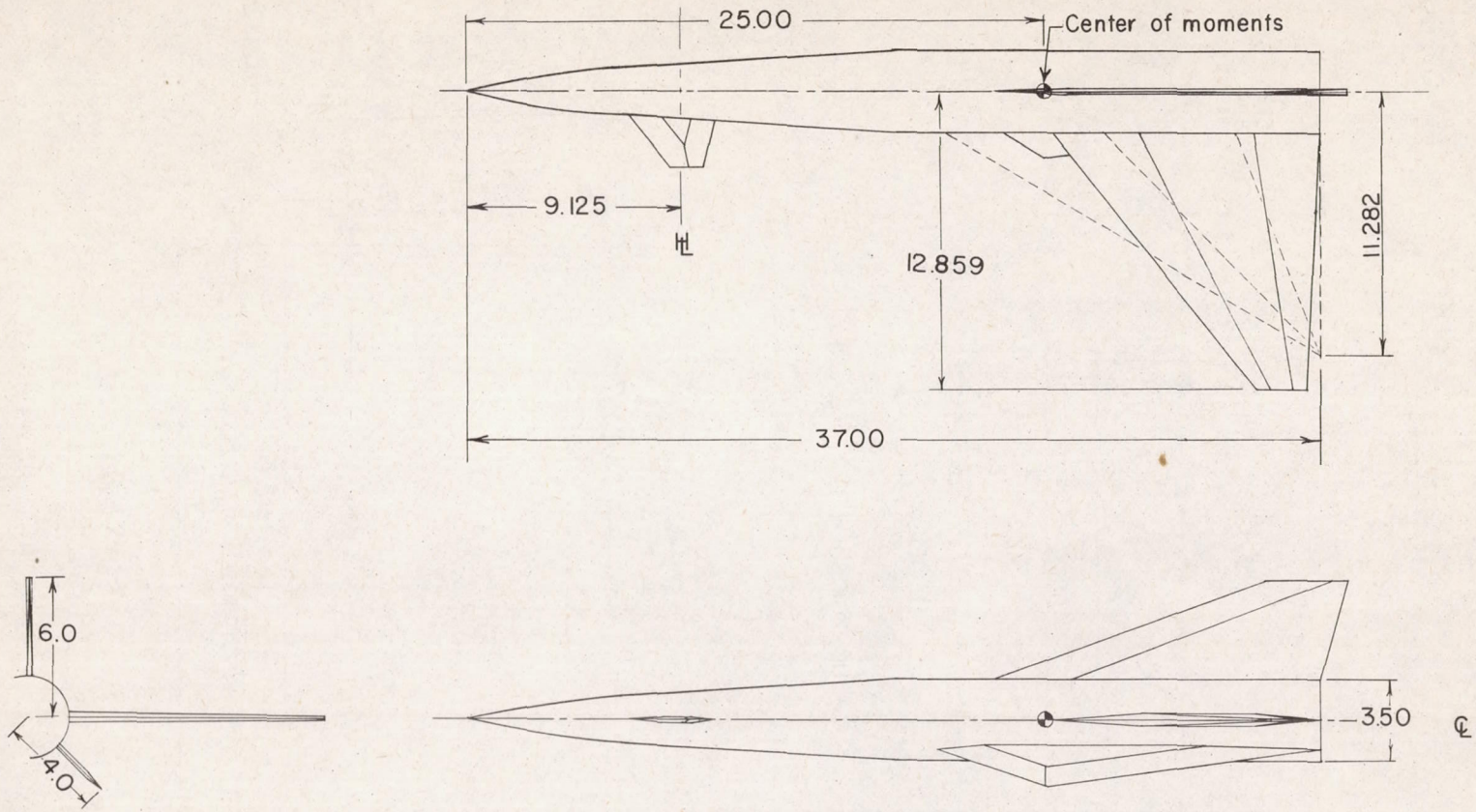
(a) Stability axis.

Figure 1.- Axes systems. (Arrows indicate positive directions.)



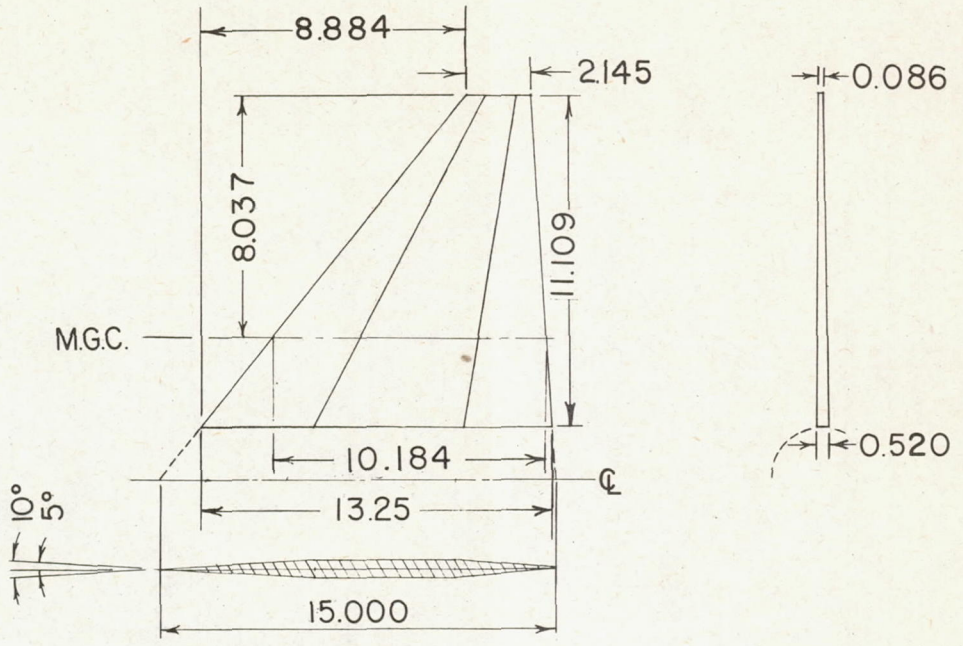
(b) Body axis.

Figure 1.- Concluded.

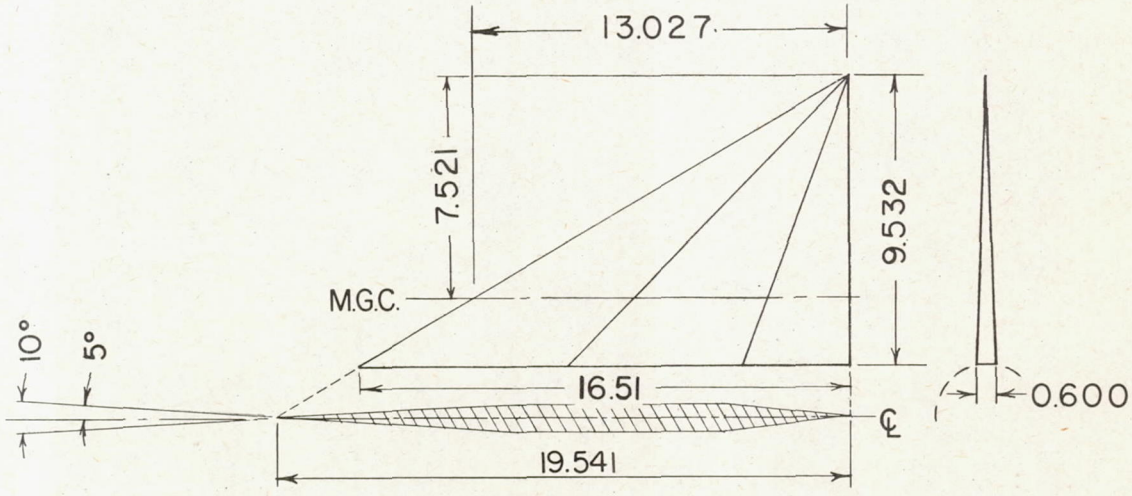


(a) Three-view drawing of model arrangement.

Figure 2.- Details of generalized canard airplane model.



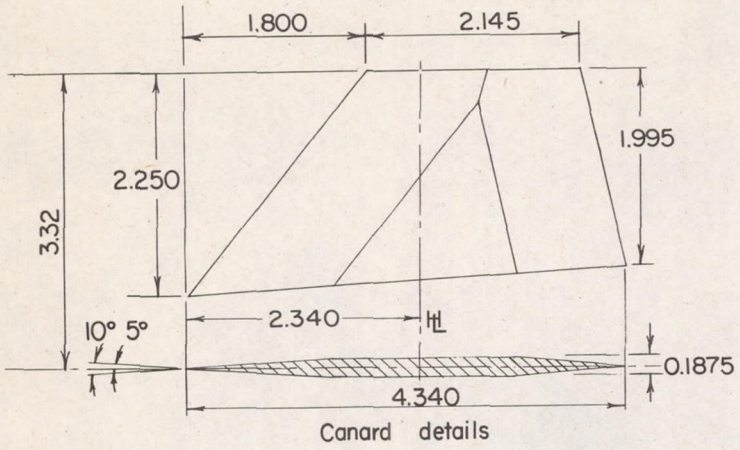
Trapezoidal wing ($\Lambda_{.80c}$=0°)



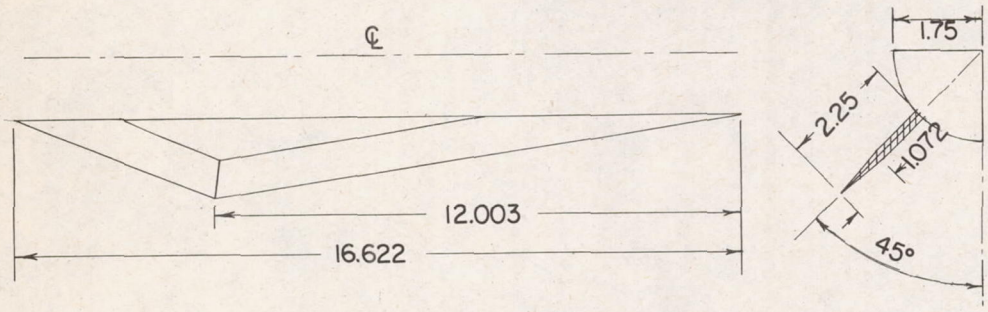
60° delta wing

(b) Details of wings.

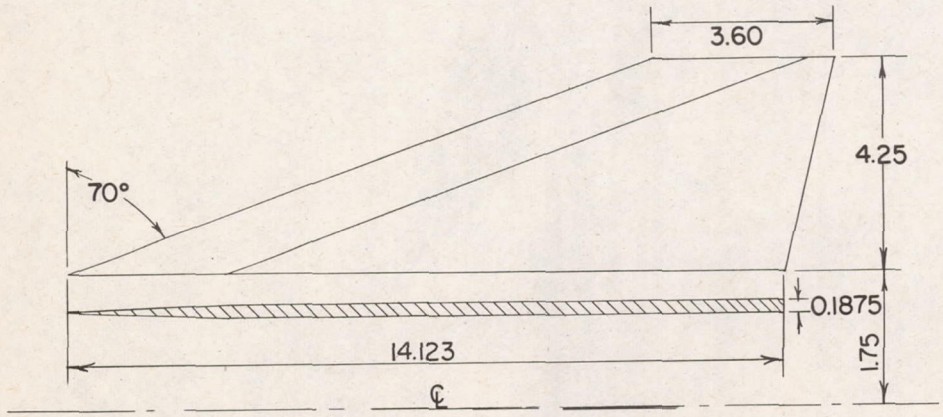
Figure 2.- Continued.



Canard details



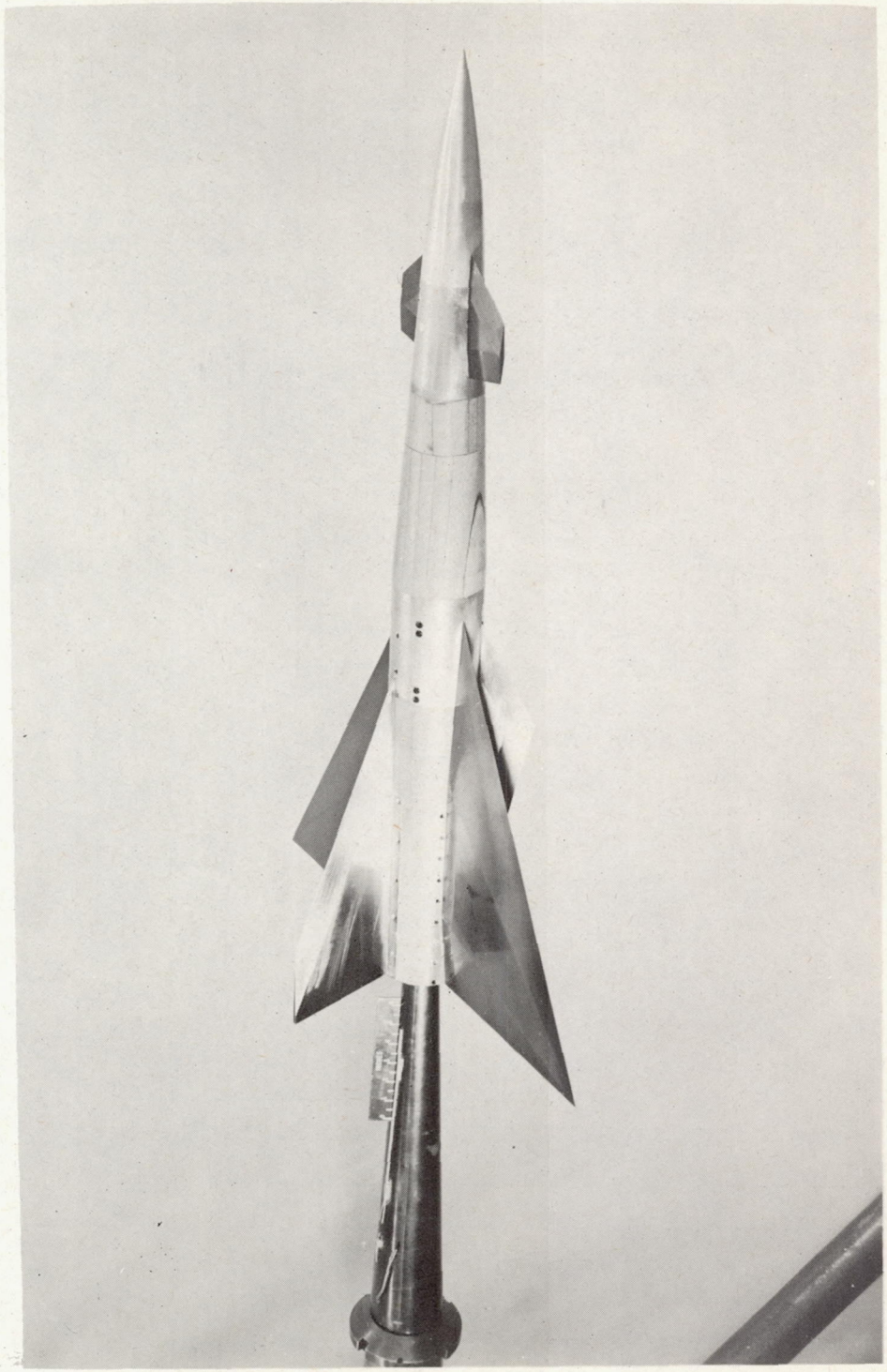
Ventral fin details



Vertical tail details

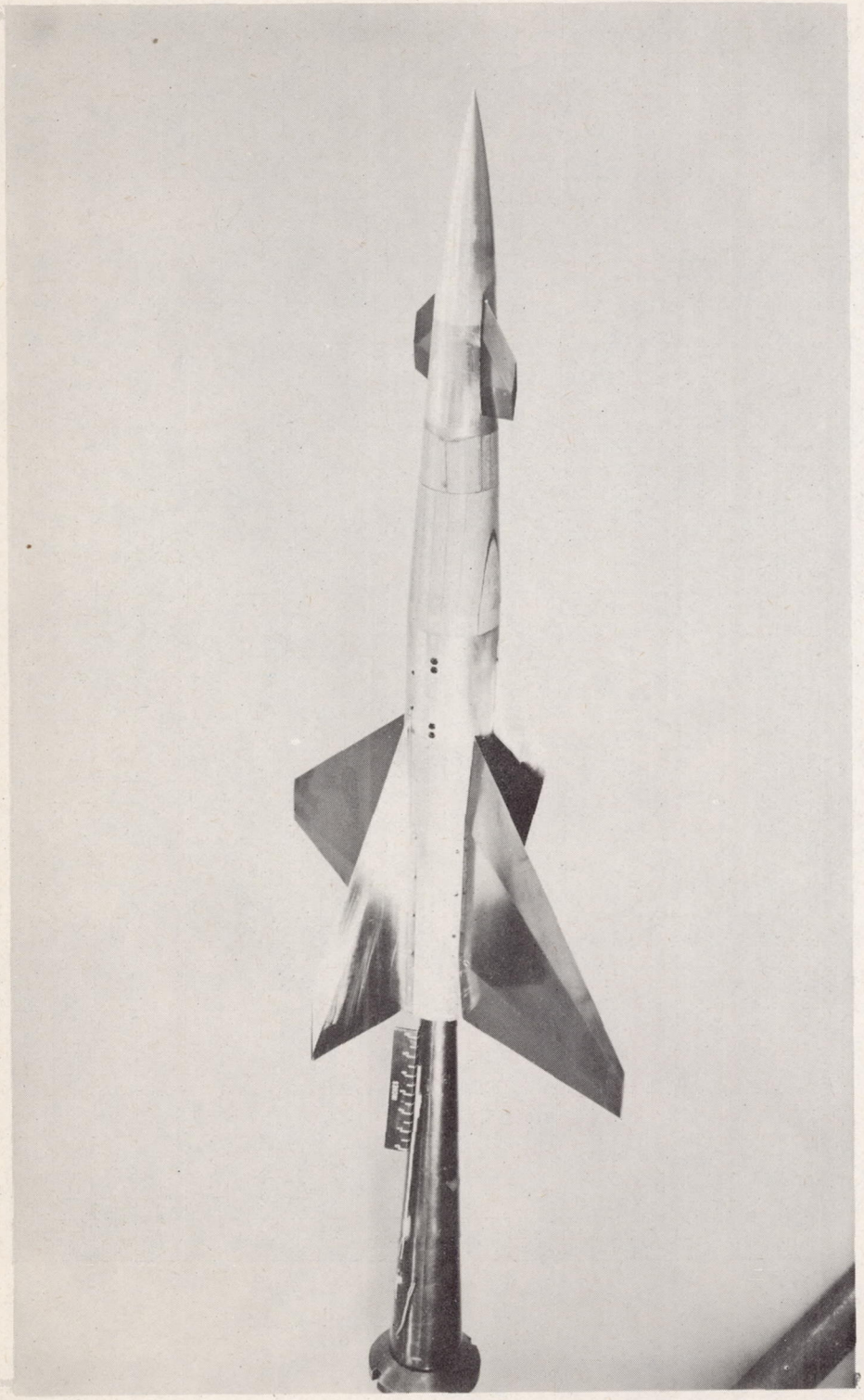
(c) Details of the canard surface, ventral fin, and vertical tail.

Figure 2.- Concluded.



(a) Delta-wing configuration. L-94460

Figure 3.- Photographs of models.



(b) Trapezoidal-wing configuration. L-94457

Figure 3.- Concluded.

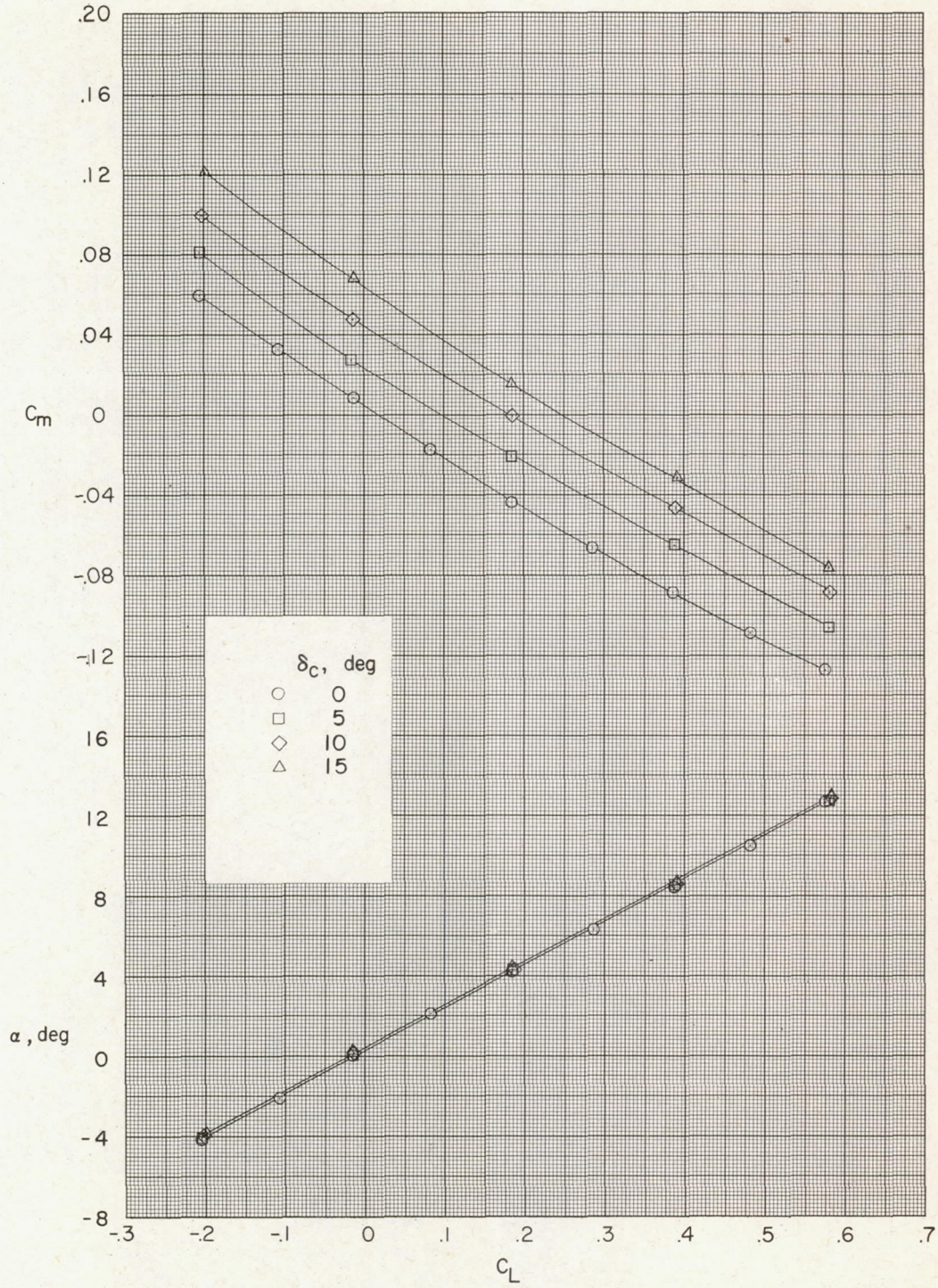


Figure 4.- The aerodynamic characteristics in pitch of the configuration with the delta wing and canards. M = 1.41.

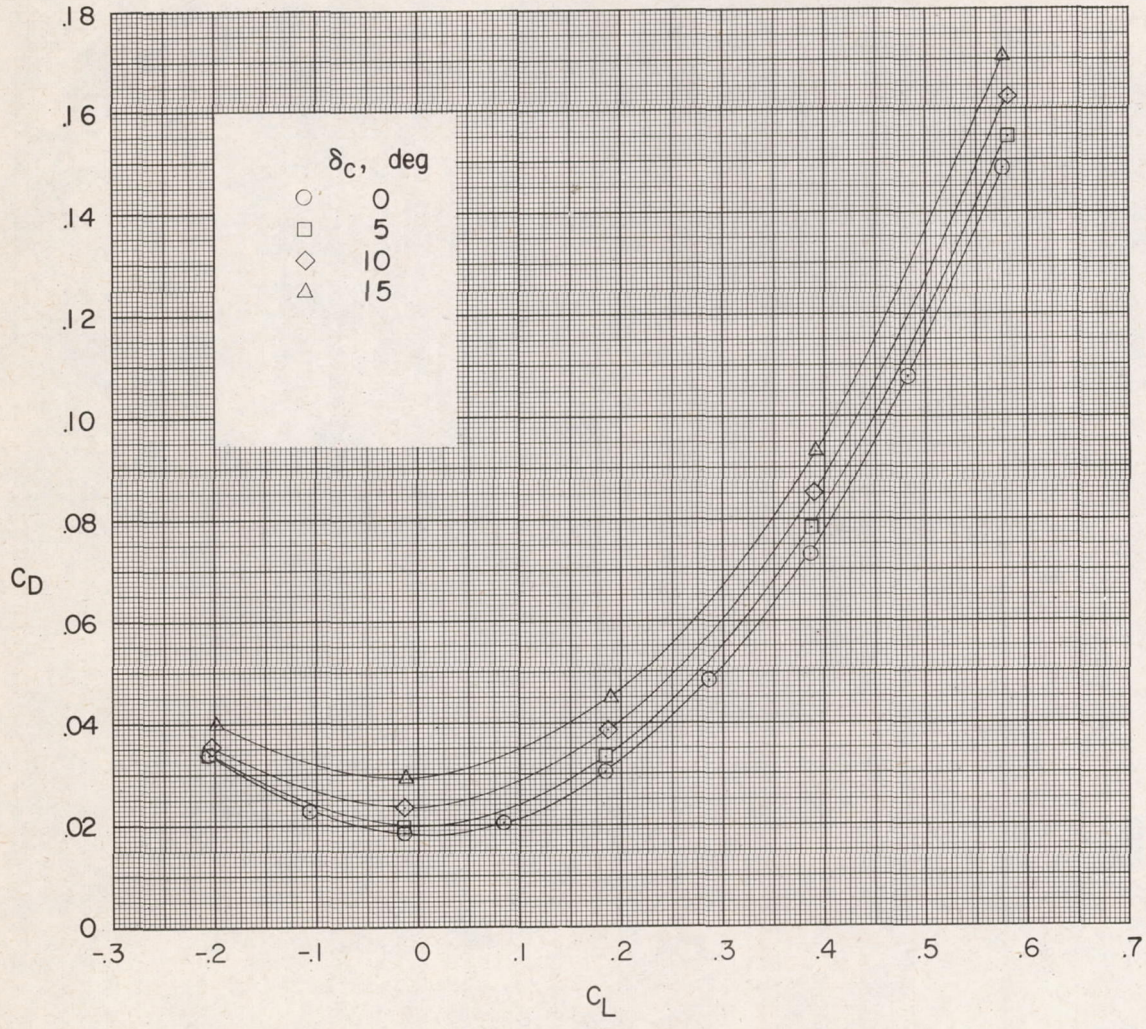


Figure 4.- Concluded.

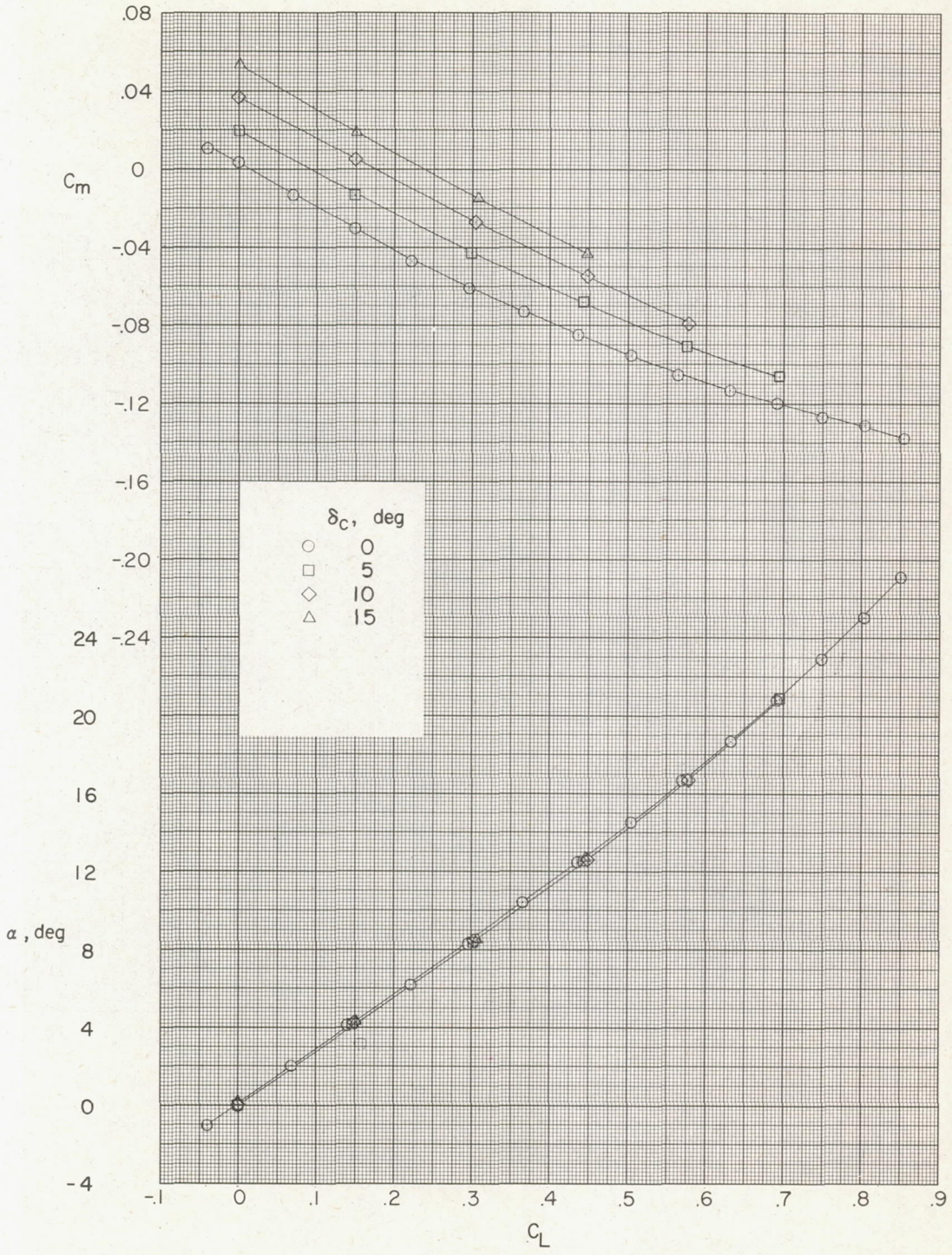


Figure 5.- The aerodynamic characteristics in pitch of the configuration with the delta wing and canards. M = 2.01.

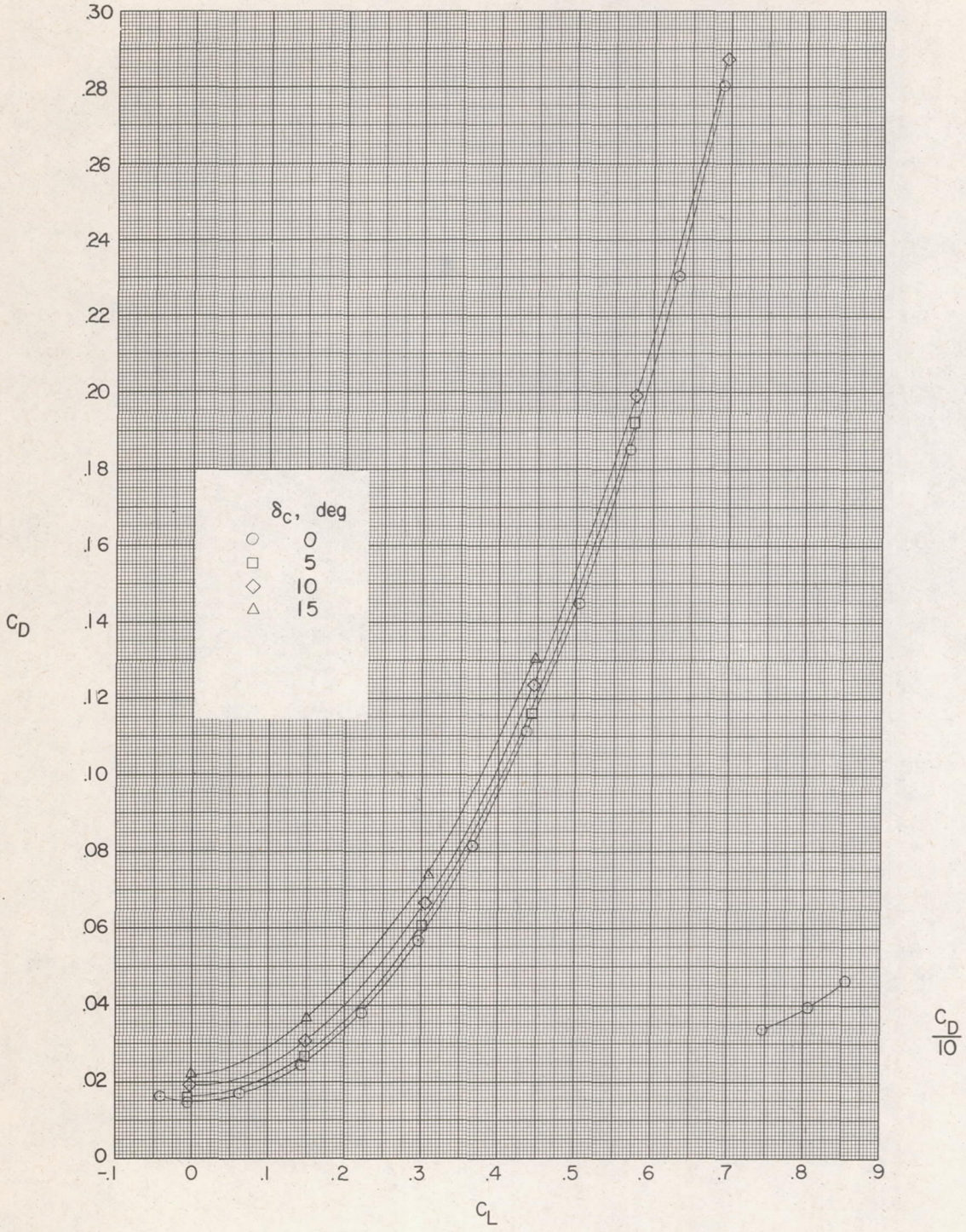


Figure 5.- Concluded.

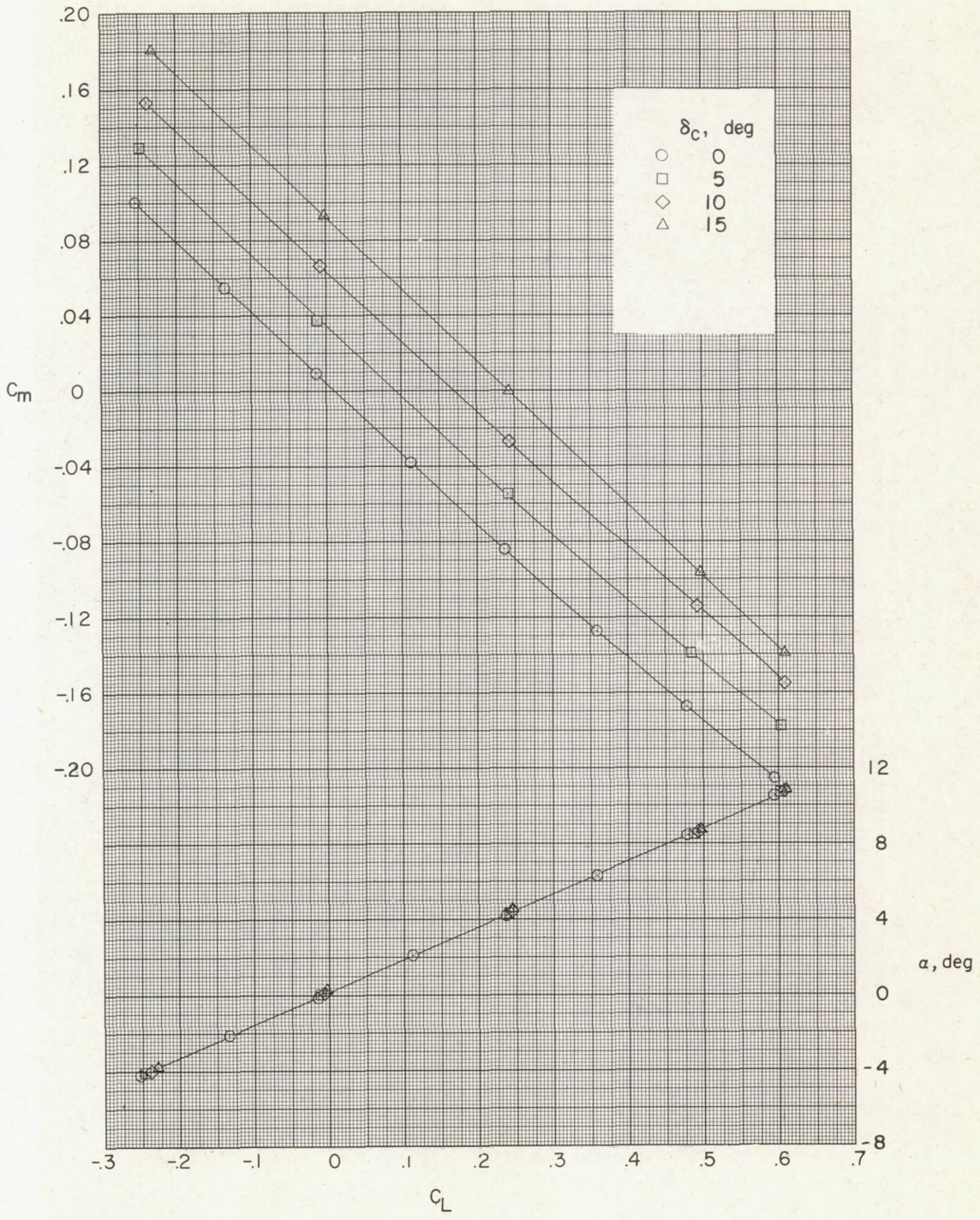


Figure 6.- The aerodynamic characteristics in pitch of the configuration with the trapezoidal wing and canards. M = 1.41.

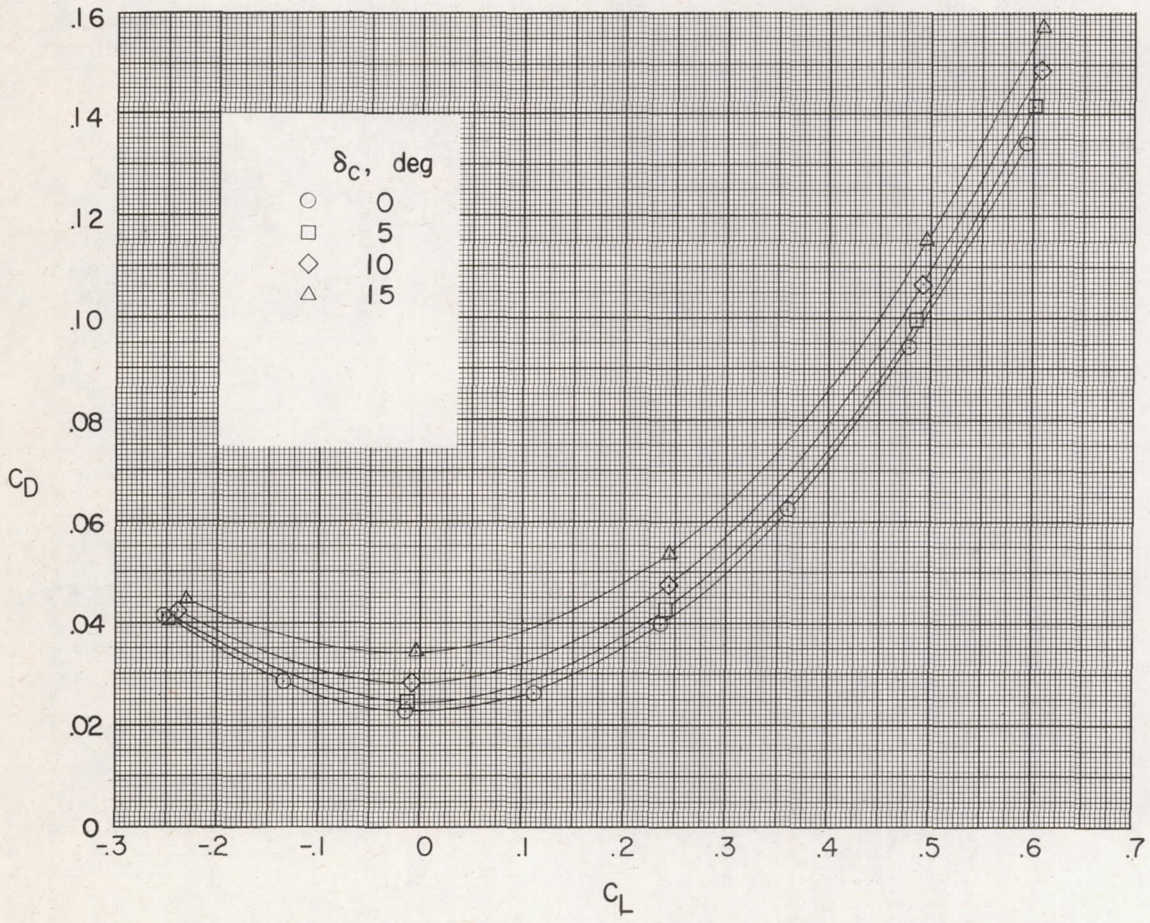


Figure 6.- Concluded.

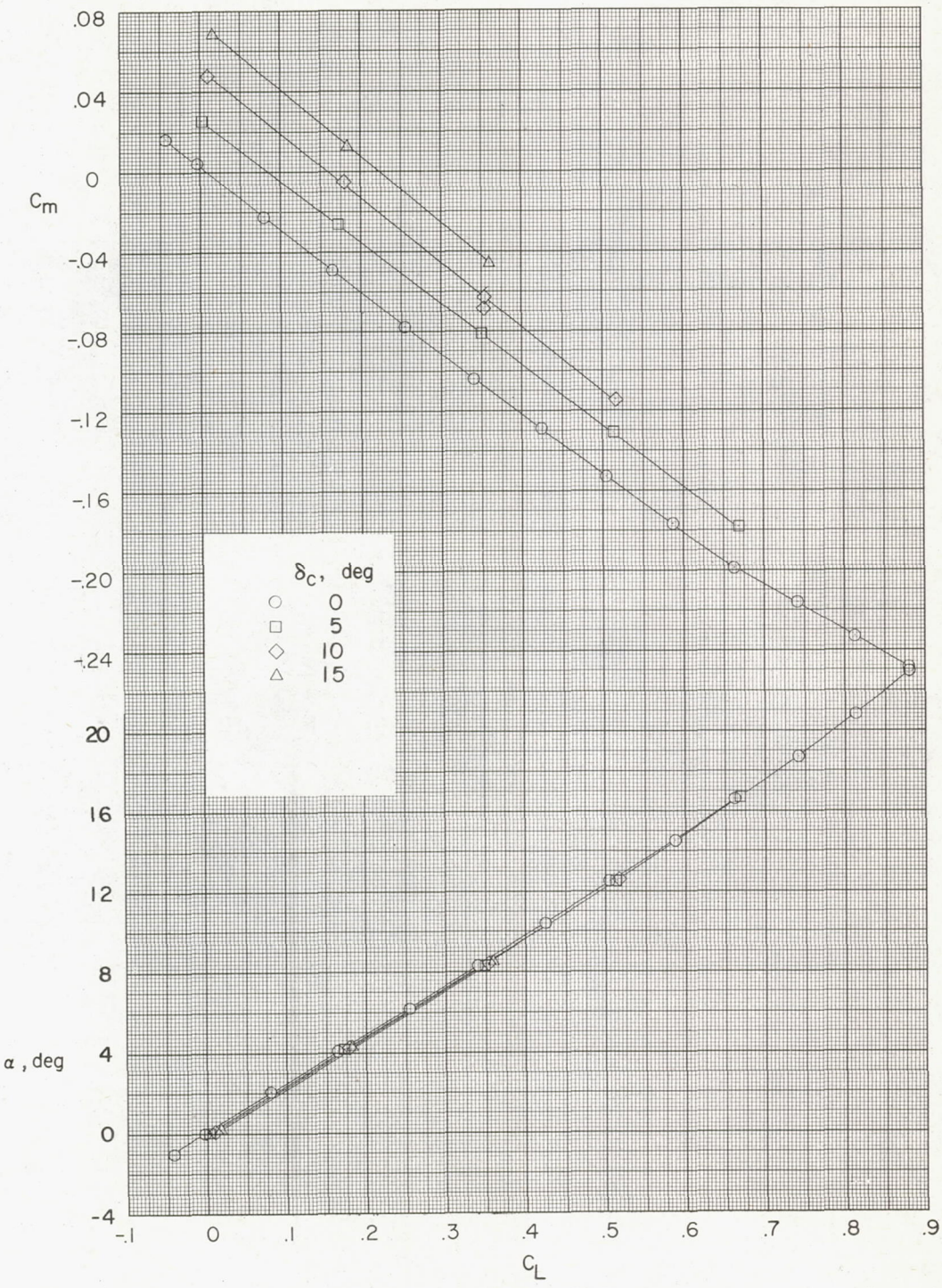


Figure 7.- The aerodynamic characteristics in pitch of the configuration with the trapezoidal wing and canards. M = 2.01.

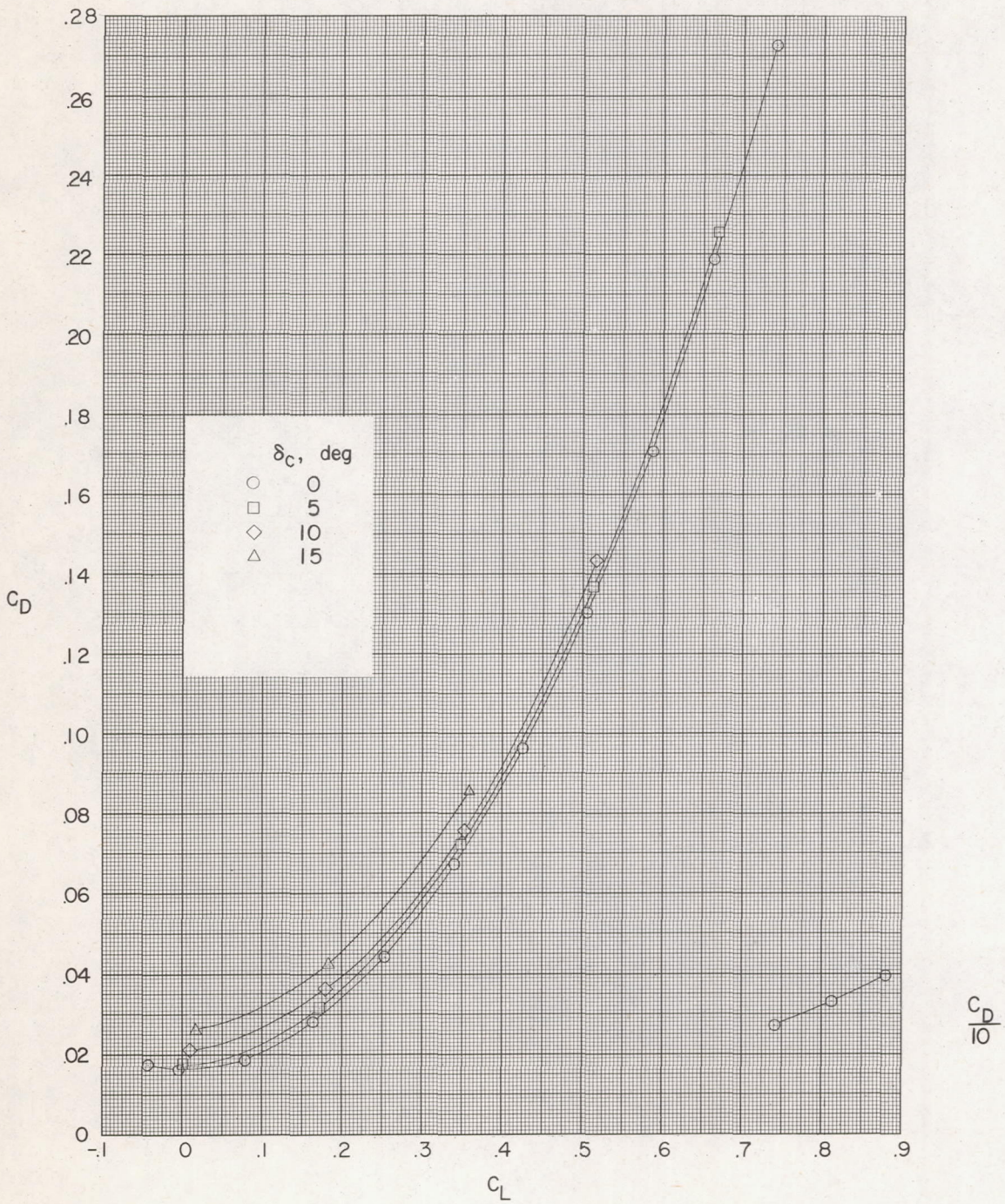
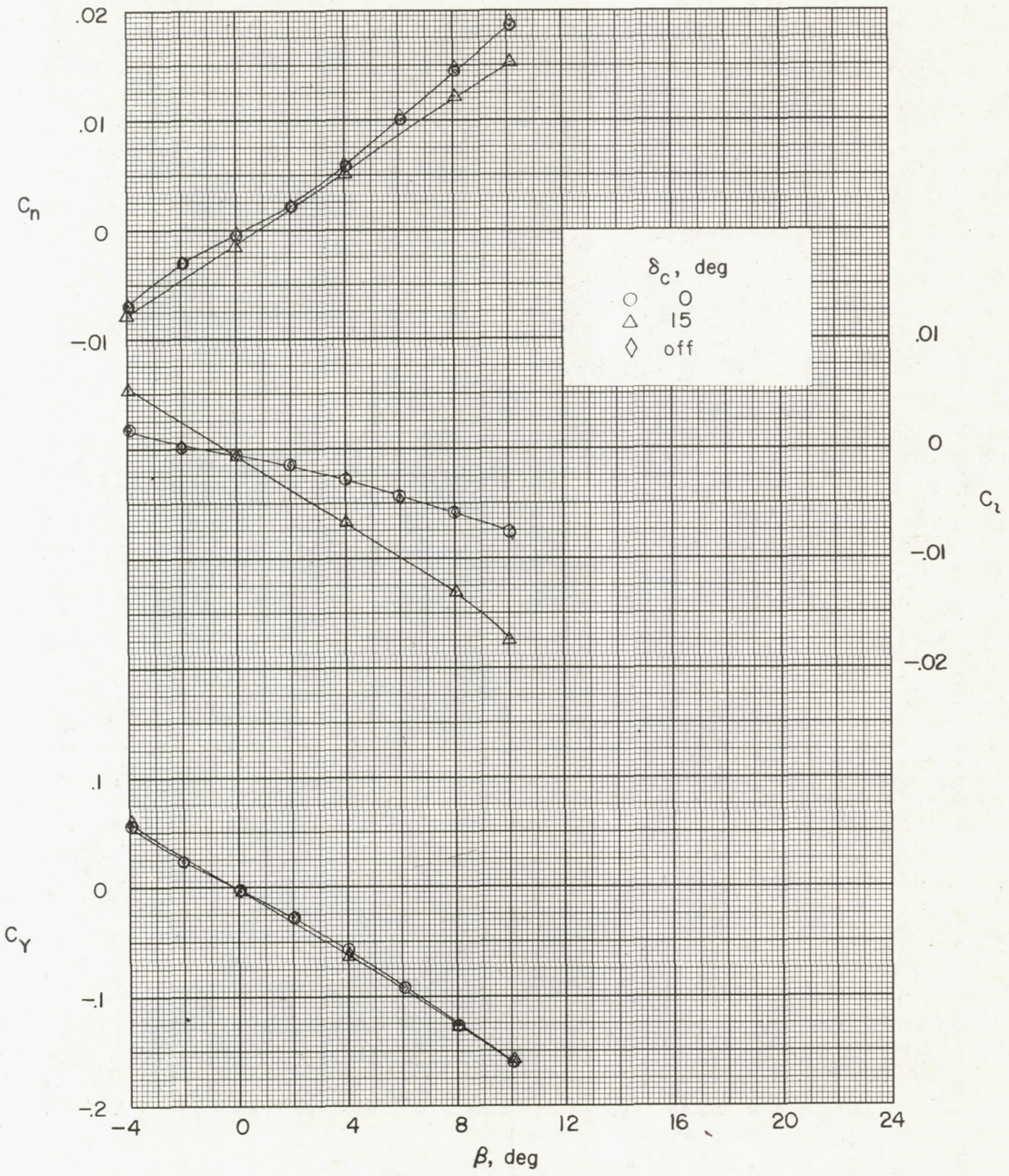
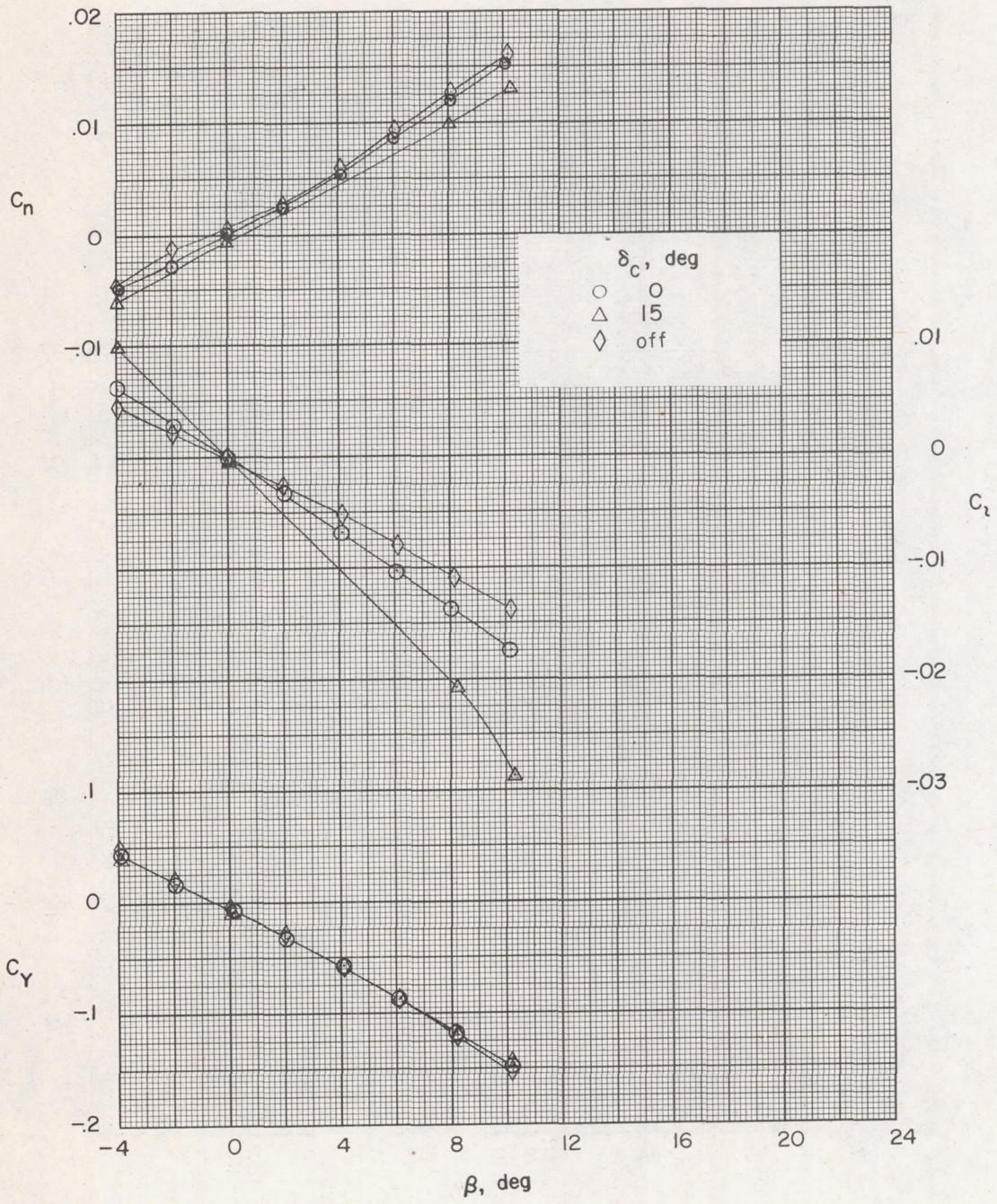


Figure 7.- Concluded.



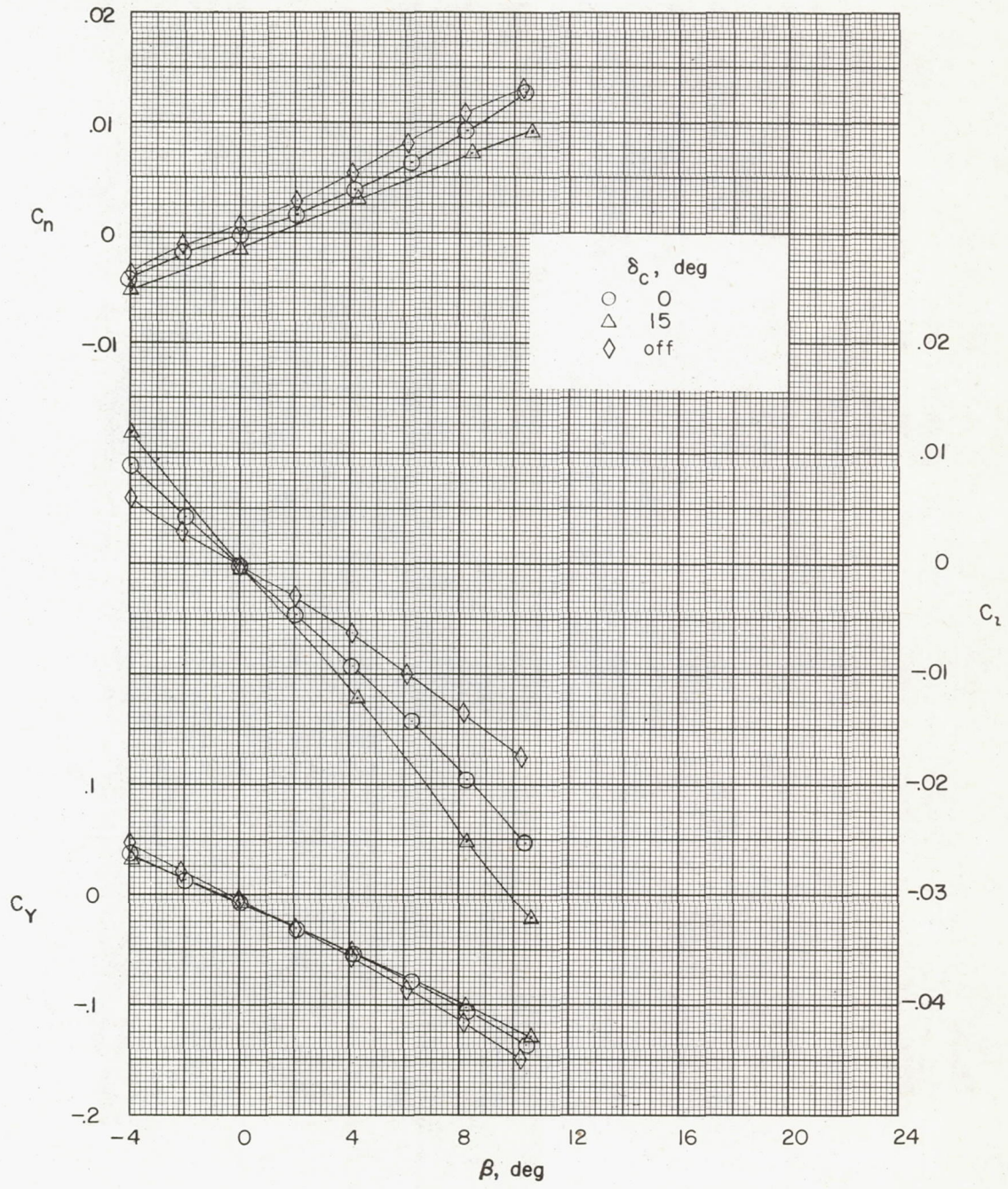
(a) $\alpha = 0^\circ$.

Figure 8.- The aerodynamic characteristics in sideslip for the configuration with the delta wing and the canards. M = 1.41.



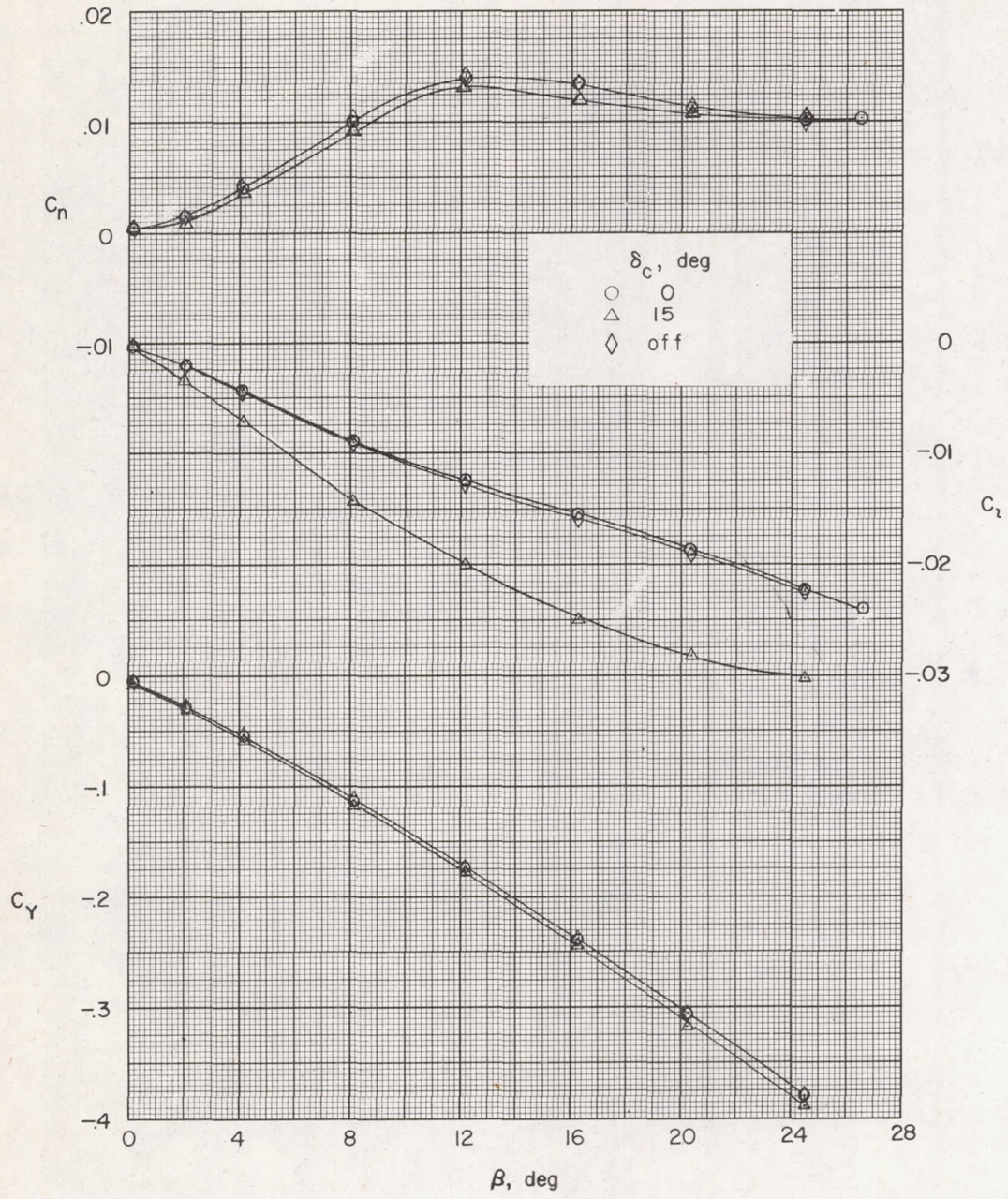
(b) $\alpha = 4.1^{\circ}$.

Figure 8.- Continued.



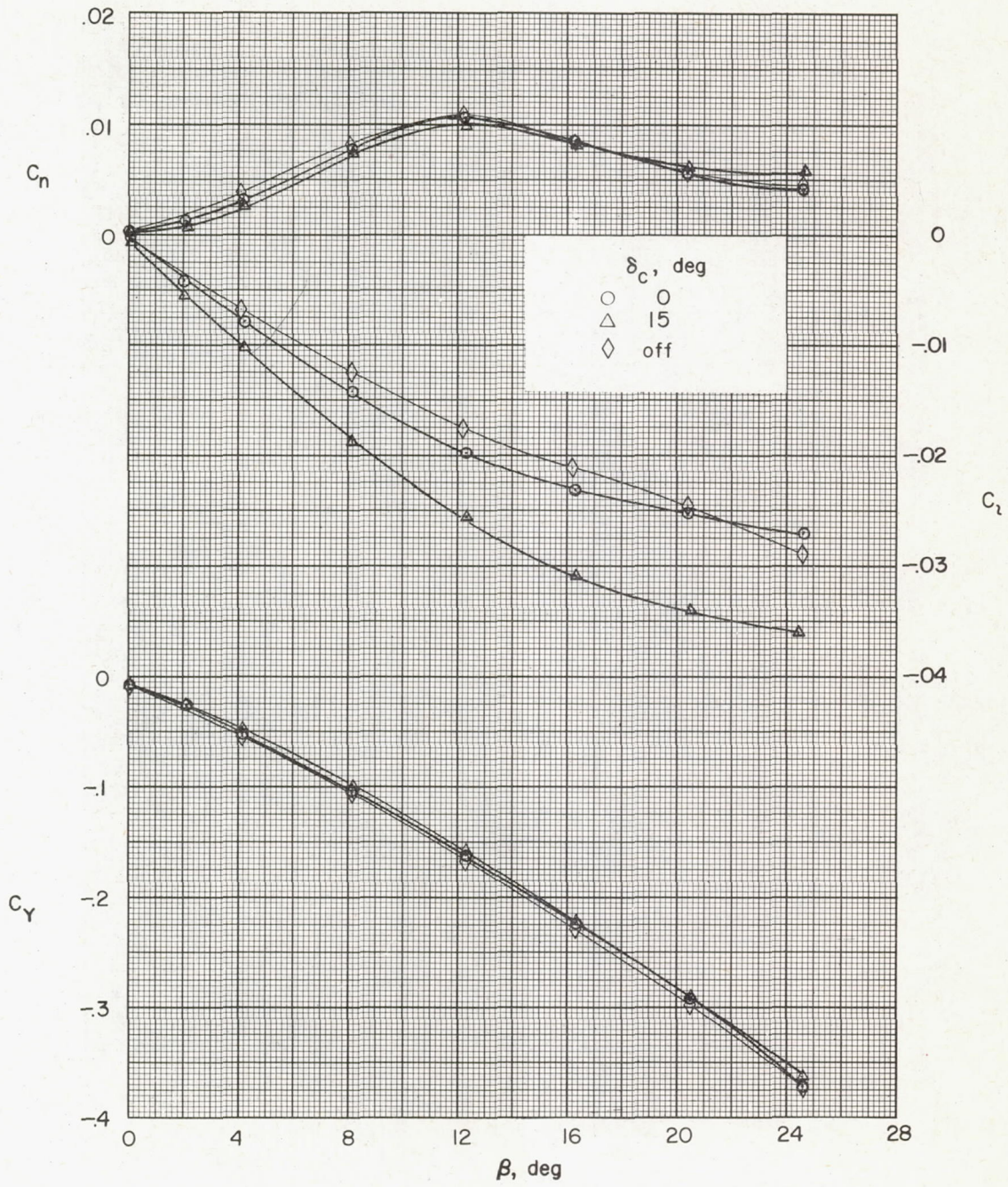
(c) $\alpha = 8.4^{\circ}$.

Figure 8.- Concluded.



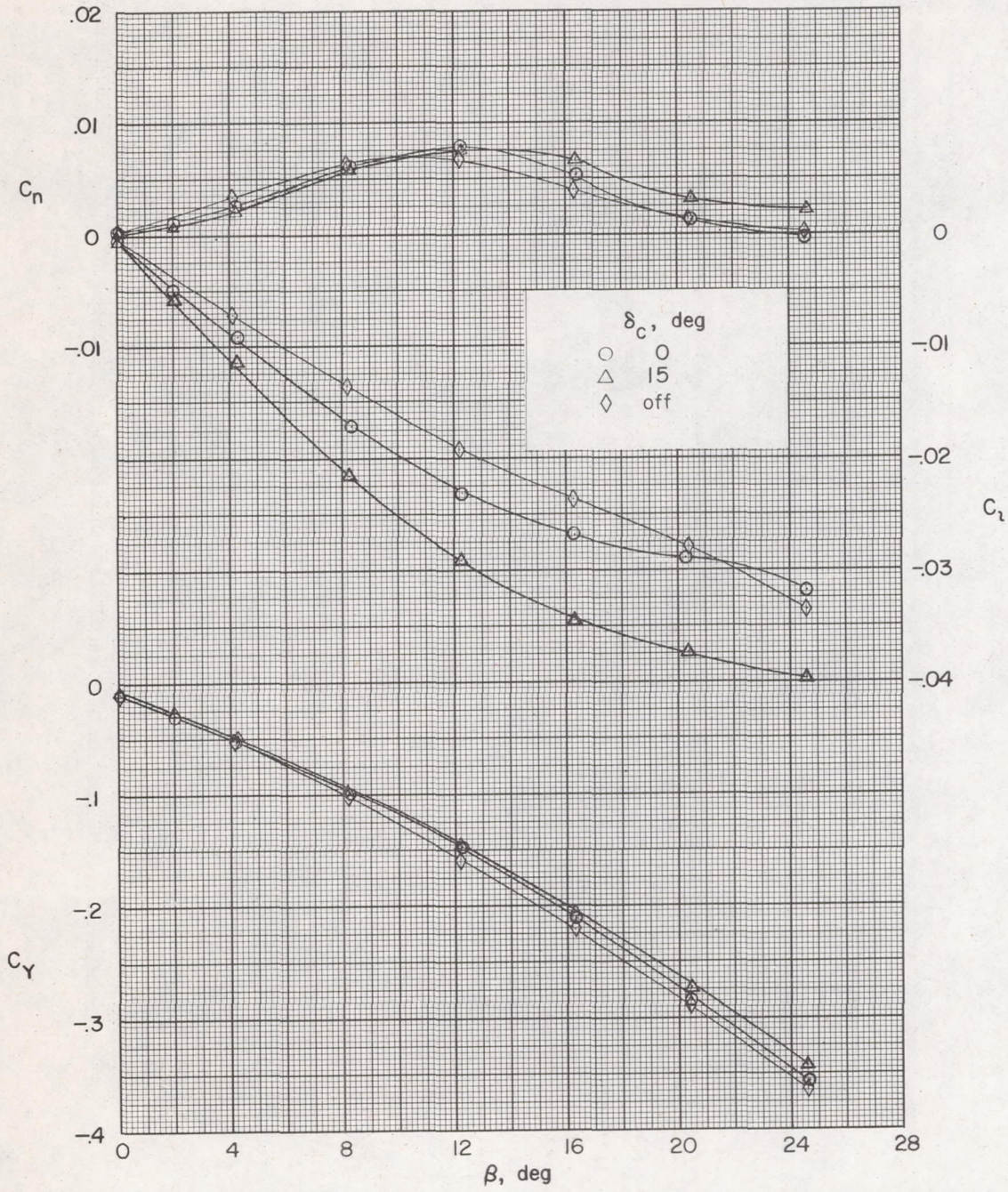
(a) $\alpha = 0^{\circ}$.

Figure 9.- The aerodynamic characteristics in sideslip for the configuration with the delta wing and the canards. M = 2.01.



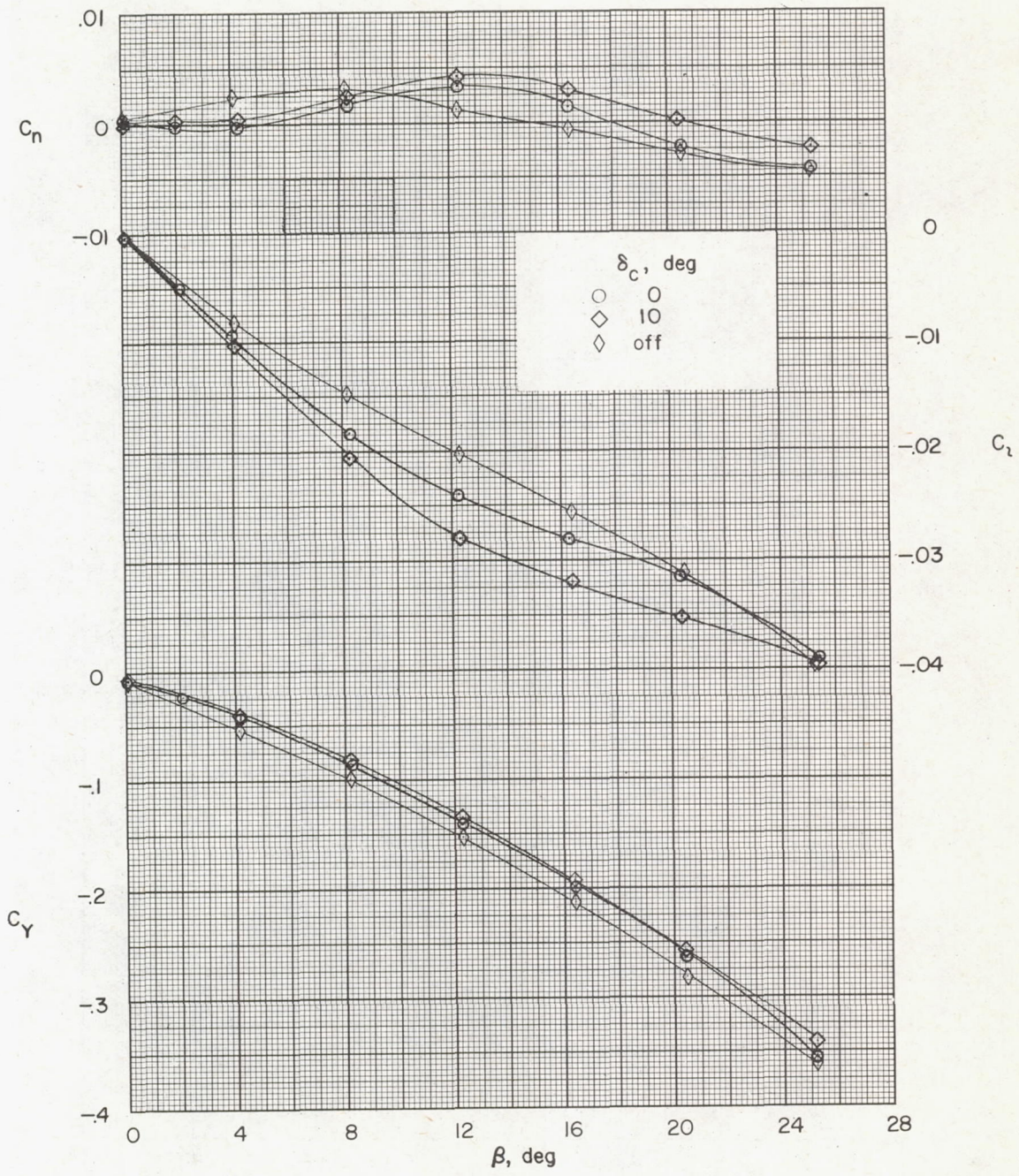
(b) $\alpha = 4.1^{\circ}$.

Figure 9.- Continued.



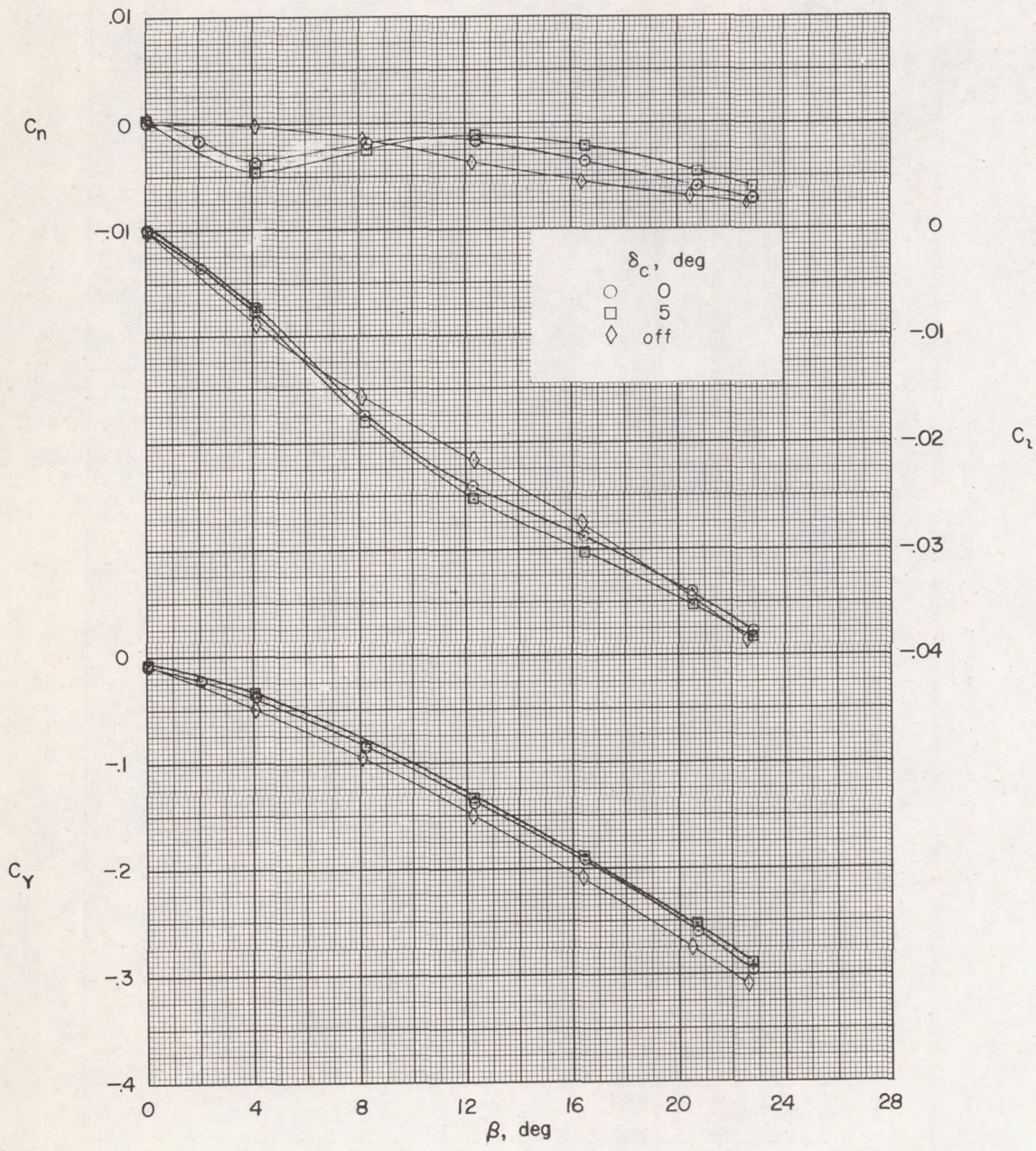
(c) $\alpha = 8.3^\circ$.

Figure 9.- Continued.



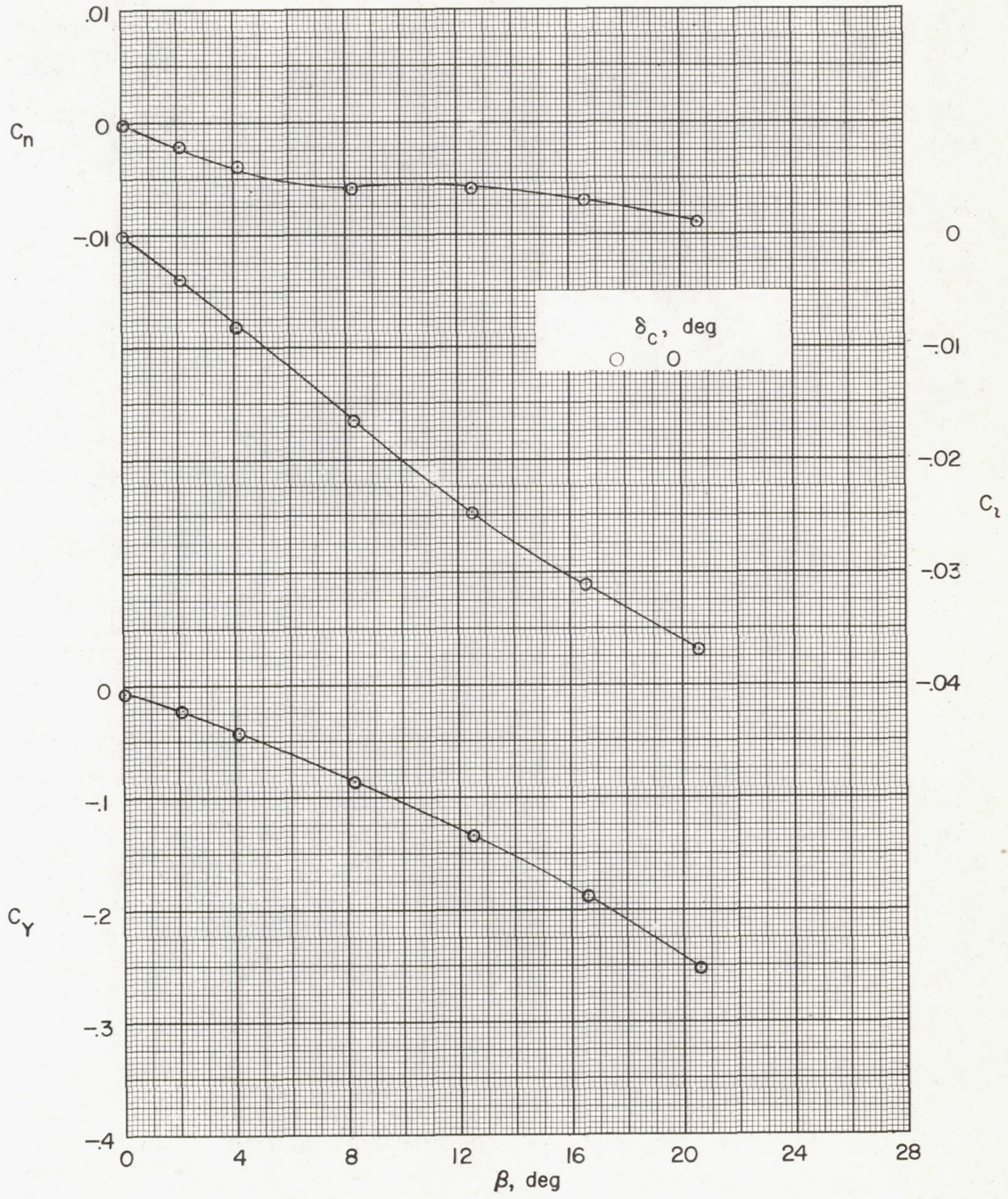
(d) $\alpha = 12.5^{\circ}$.

Figure 9.- Continued.



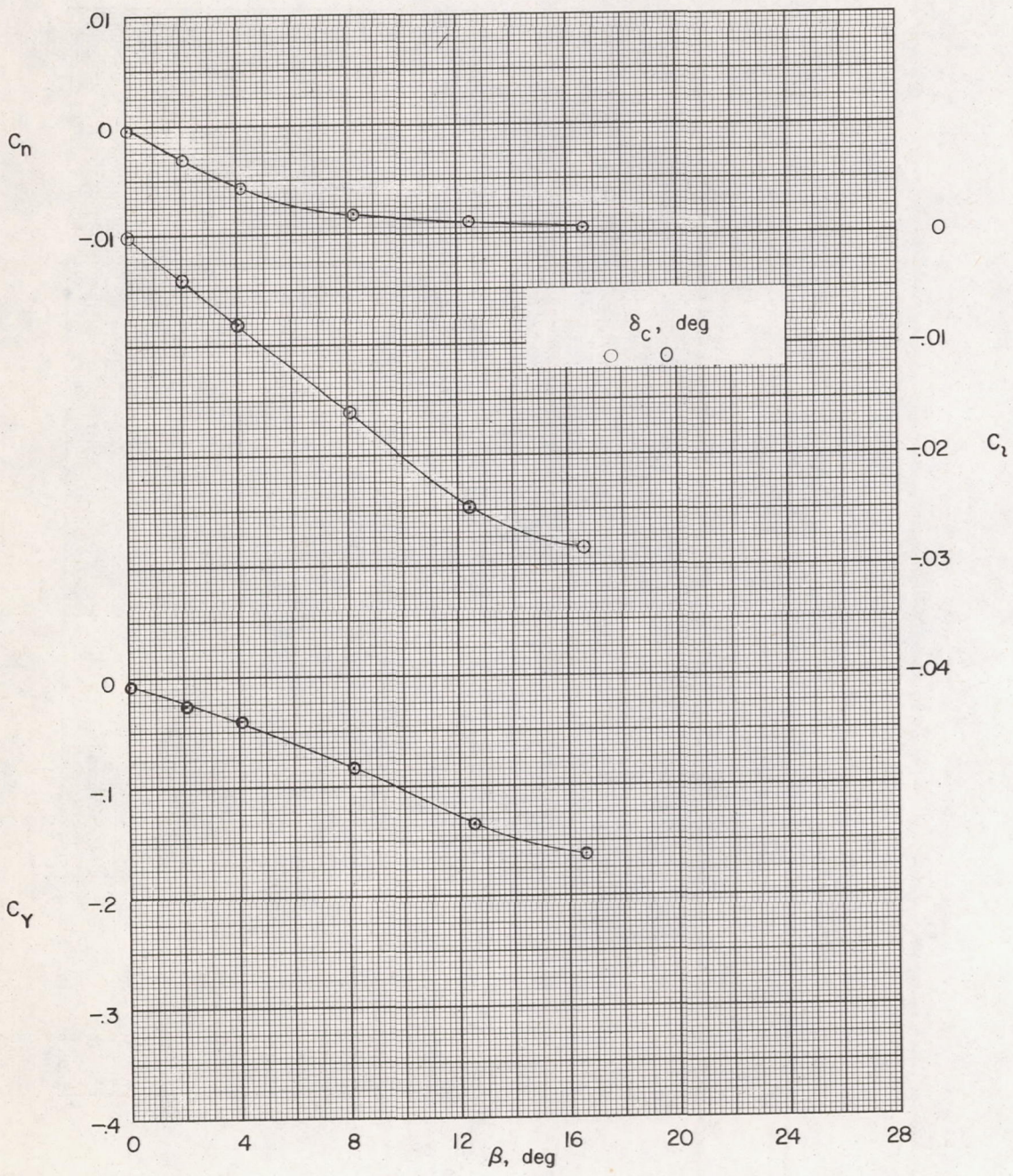
(e) $\alpha = 16.6^{\circ}$.

Figure 9.- Continued.



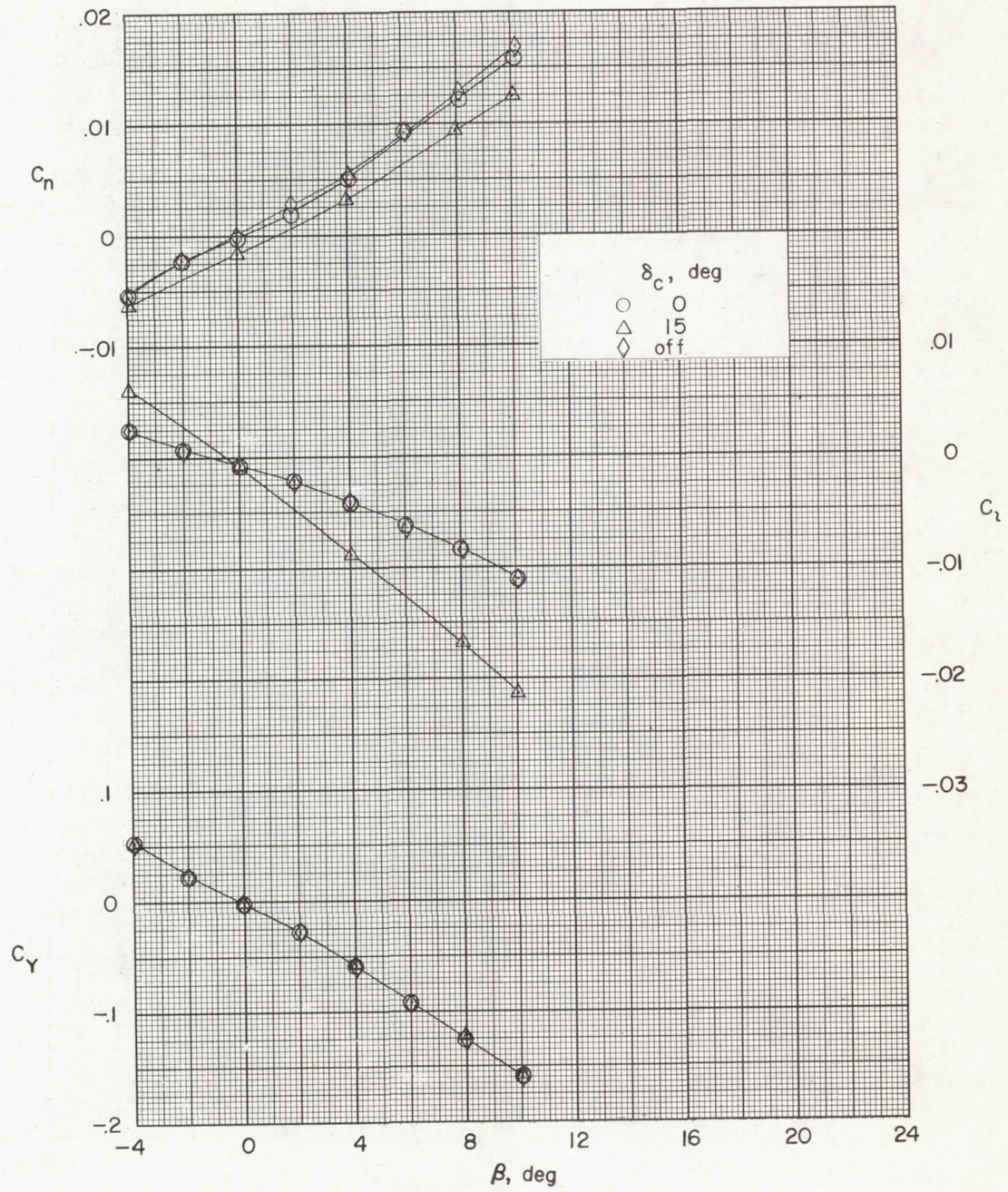
(f) $\alpha = 20.8^{\circ}$.

Figure 9.- Continued.



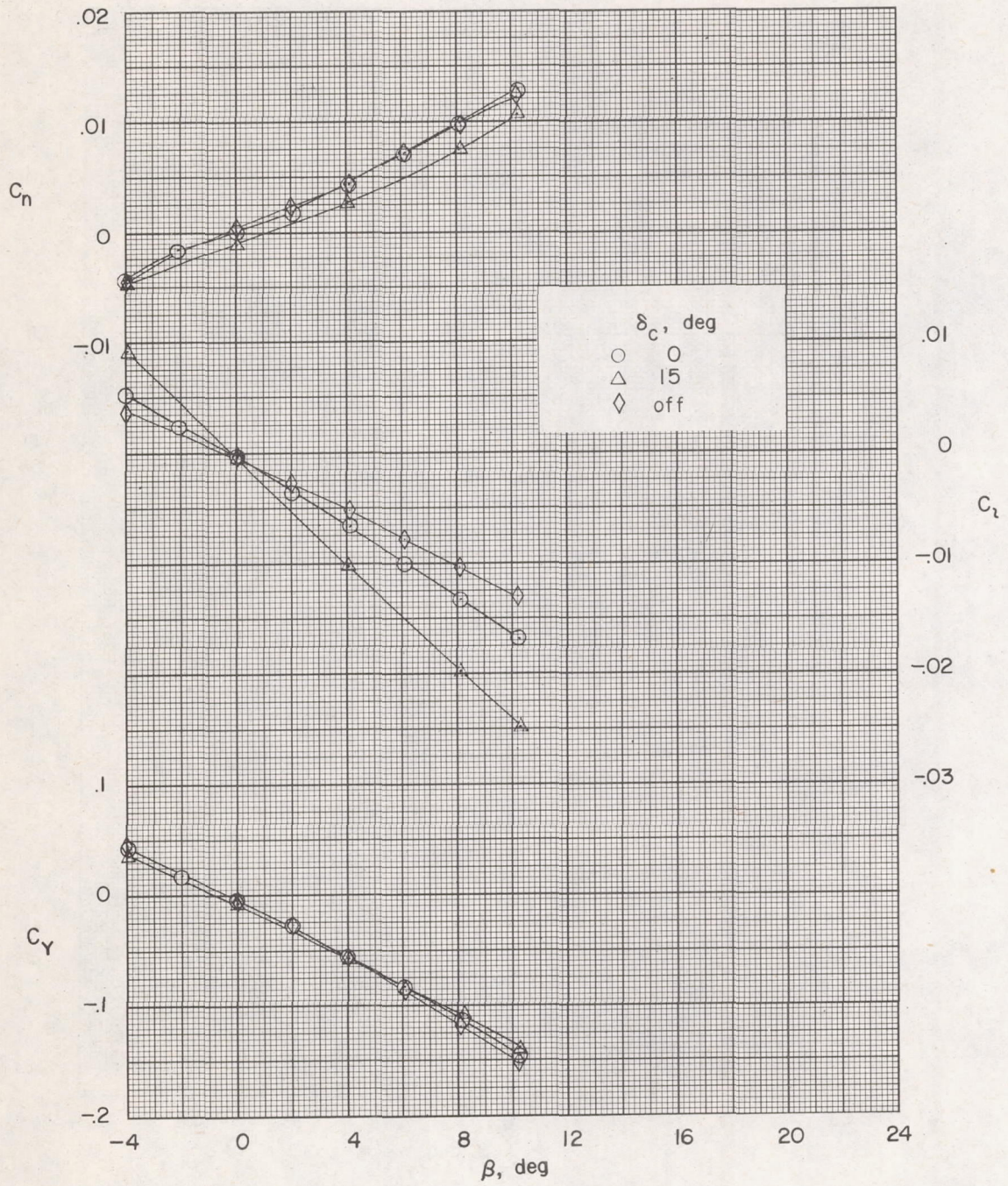
(g) $\alpha = 25^{\circ}$.

Figure 9.- Concluded.



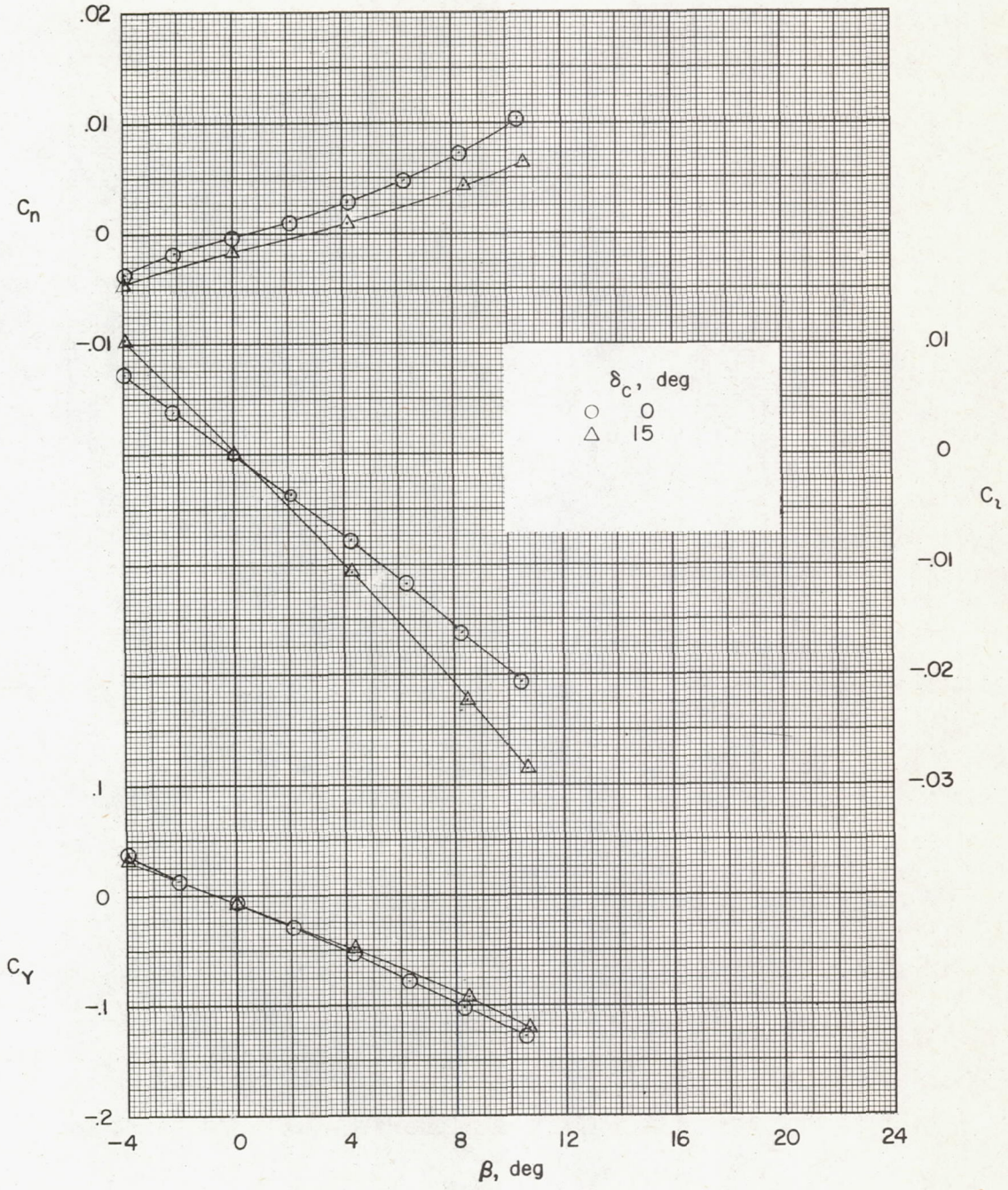
(a) $\alpha = 0^{\circ}$.

Figure 10.- The aerodynamic characteristics in sideslip of the configuration with the trapezoidal wing and the canards. M = 1.41.



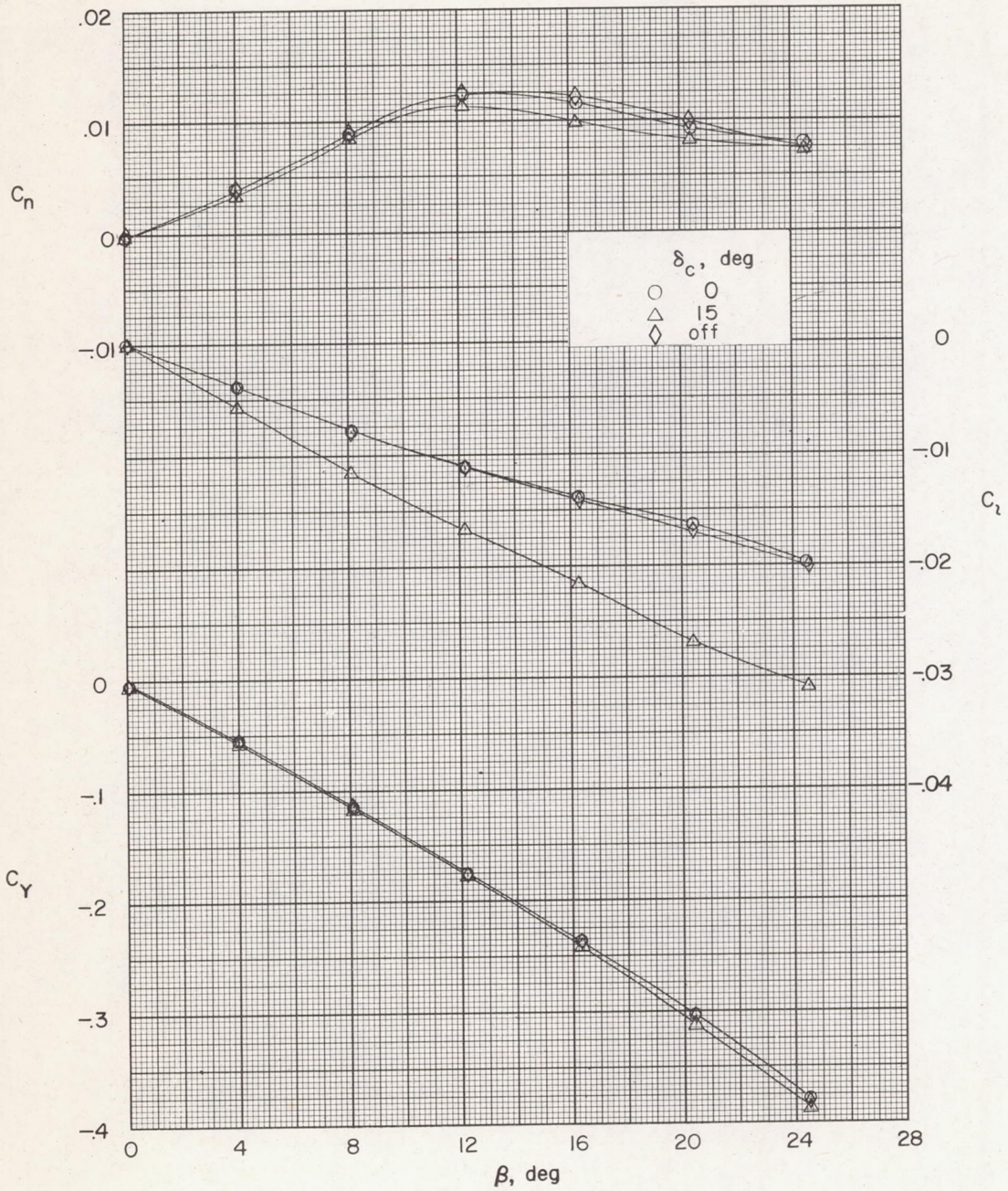
(b) $\alpha = 4.2^{\circ}$.

Figure 10.- Continued.



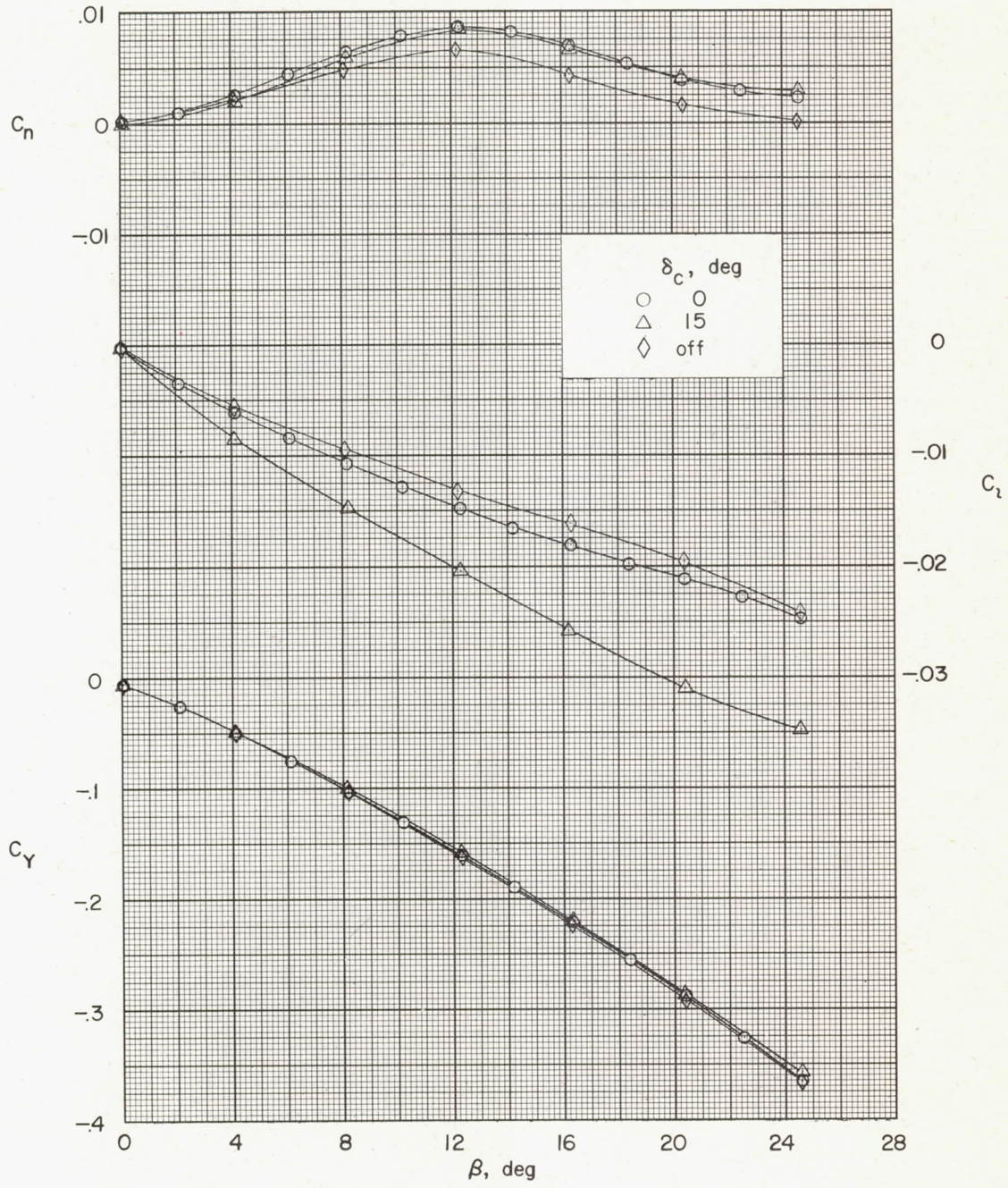
(c) $\alpha = 8.4^{\circ}$.

Figure 10.- Concluded.



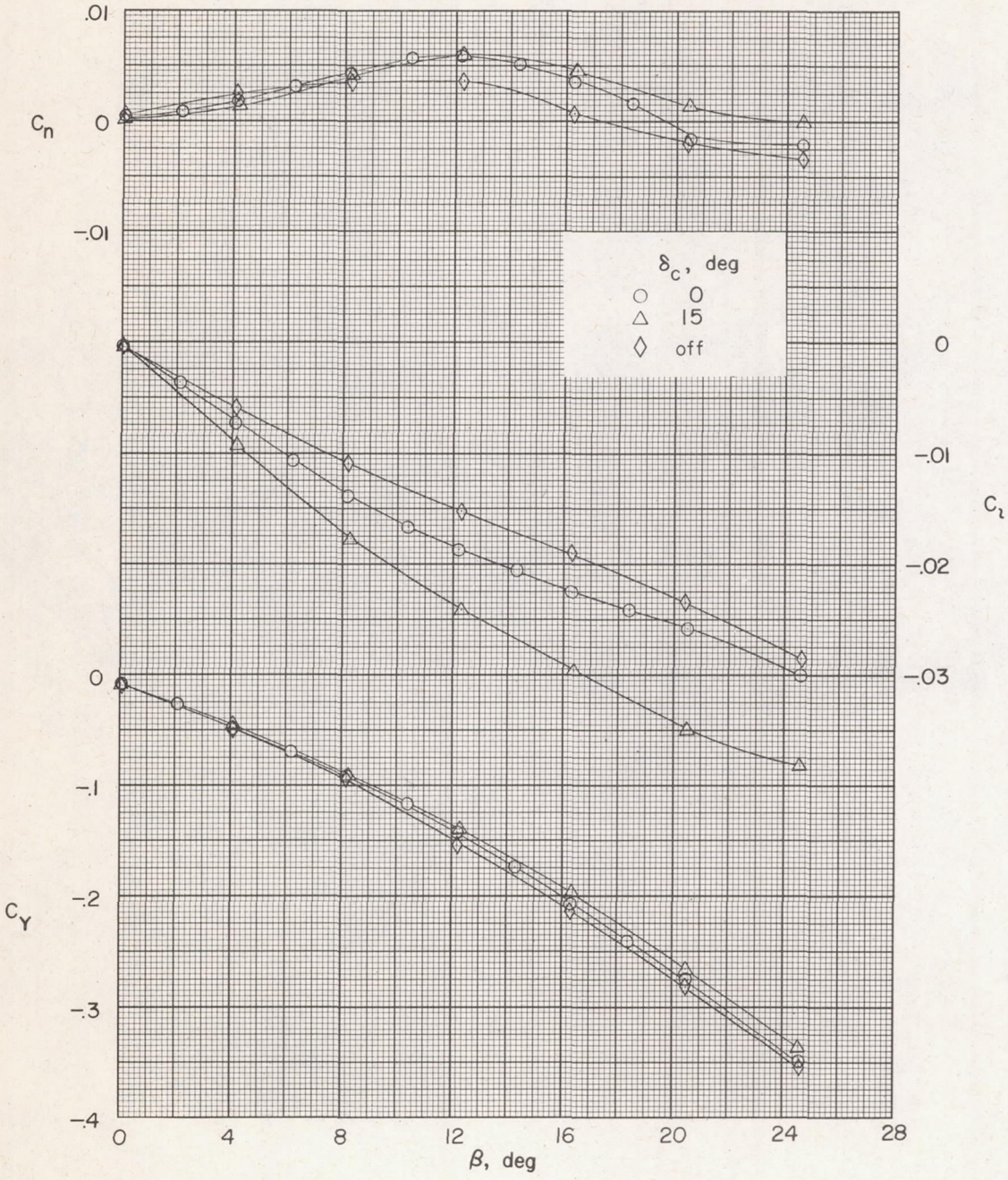
(a) $\alpha = 0^{\circ}$.

Figure 11.- The aerodynamic characteristics in sideslip of the configuration with the trapezoidal wing and the canards. M = 2.01.



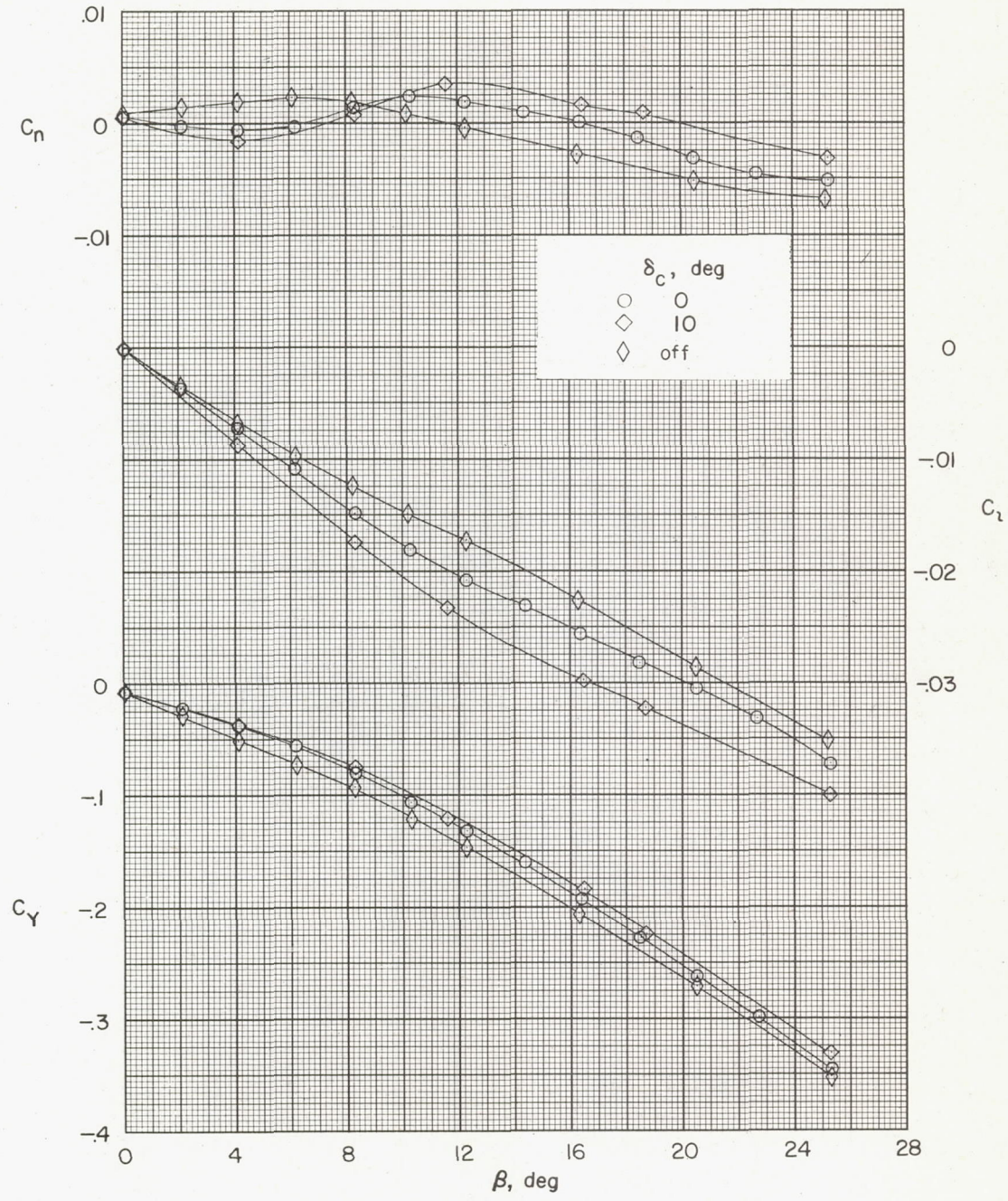
(b) $\alpha = 4.1^{\circ}$.

Figure 11.- Continued.



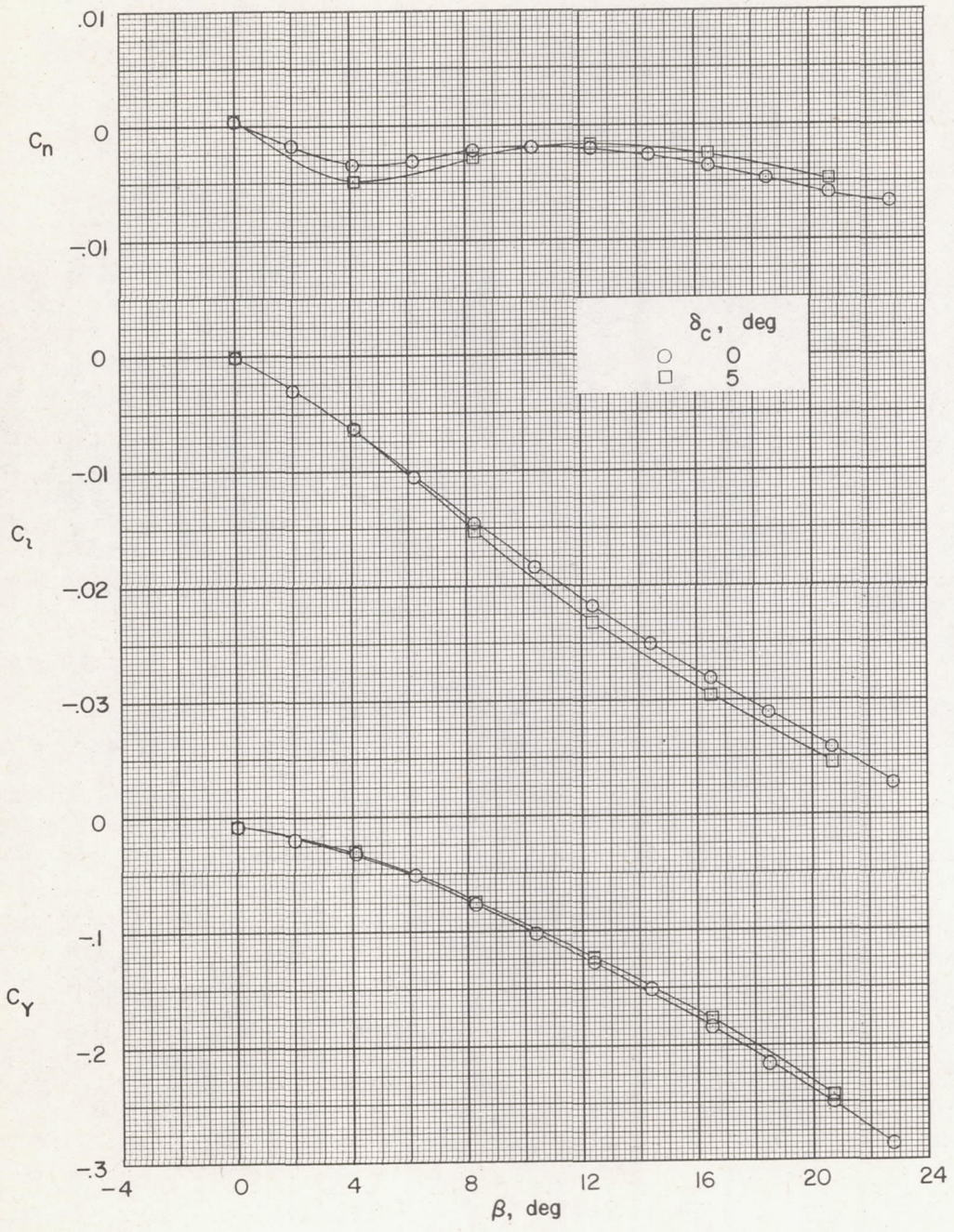
(c) $\alpha = 8.3^\circ$.

Figure 11.- Continued.



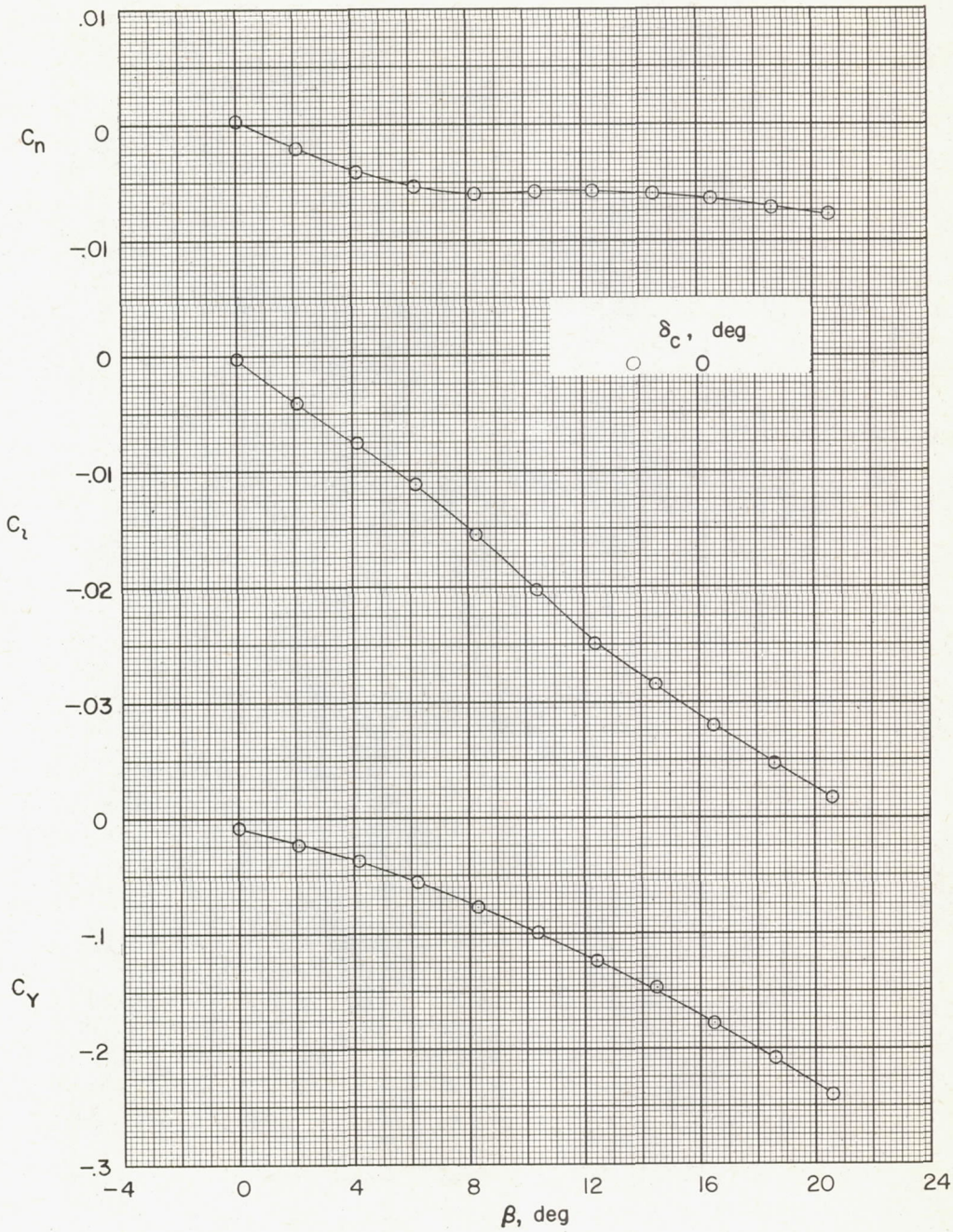
(d) $\alpha = 12.5^{\circ}$.

Figure 11.- Continued.



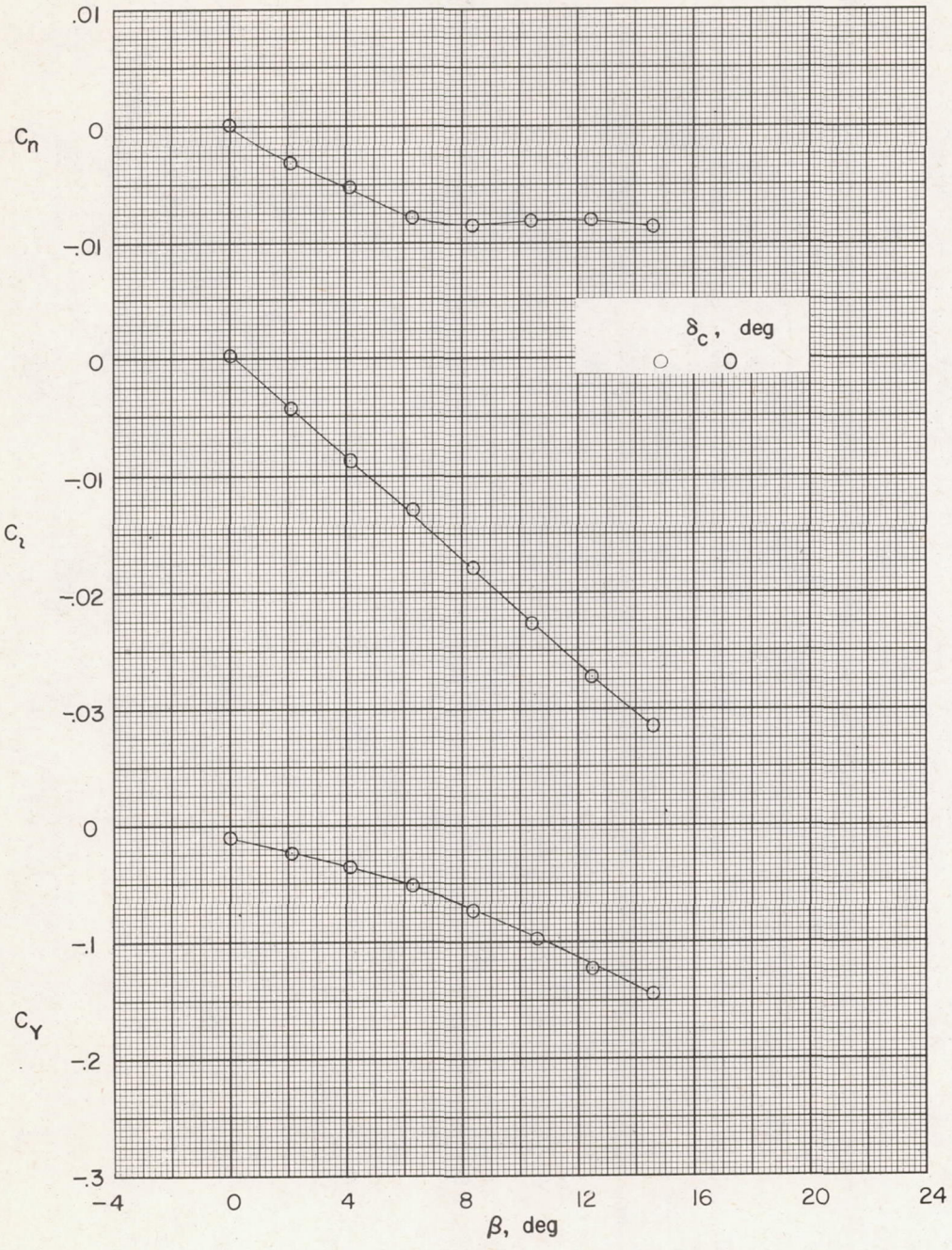
(e) $\alpha = 16.6^{\circ}$.

Figure 11.- Continued.



(f) $\alpha = 20.8^{\circ}$.

Figure 11.- Continued.



(g) $\alpha = 25^{\circ}$.

Figure 11.- Concluded.

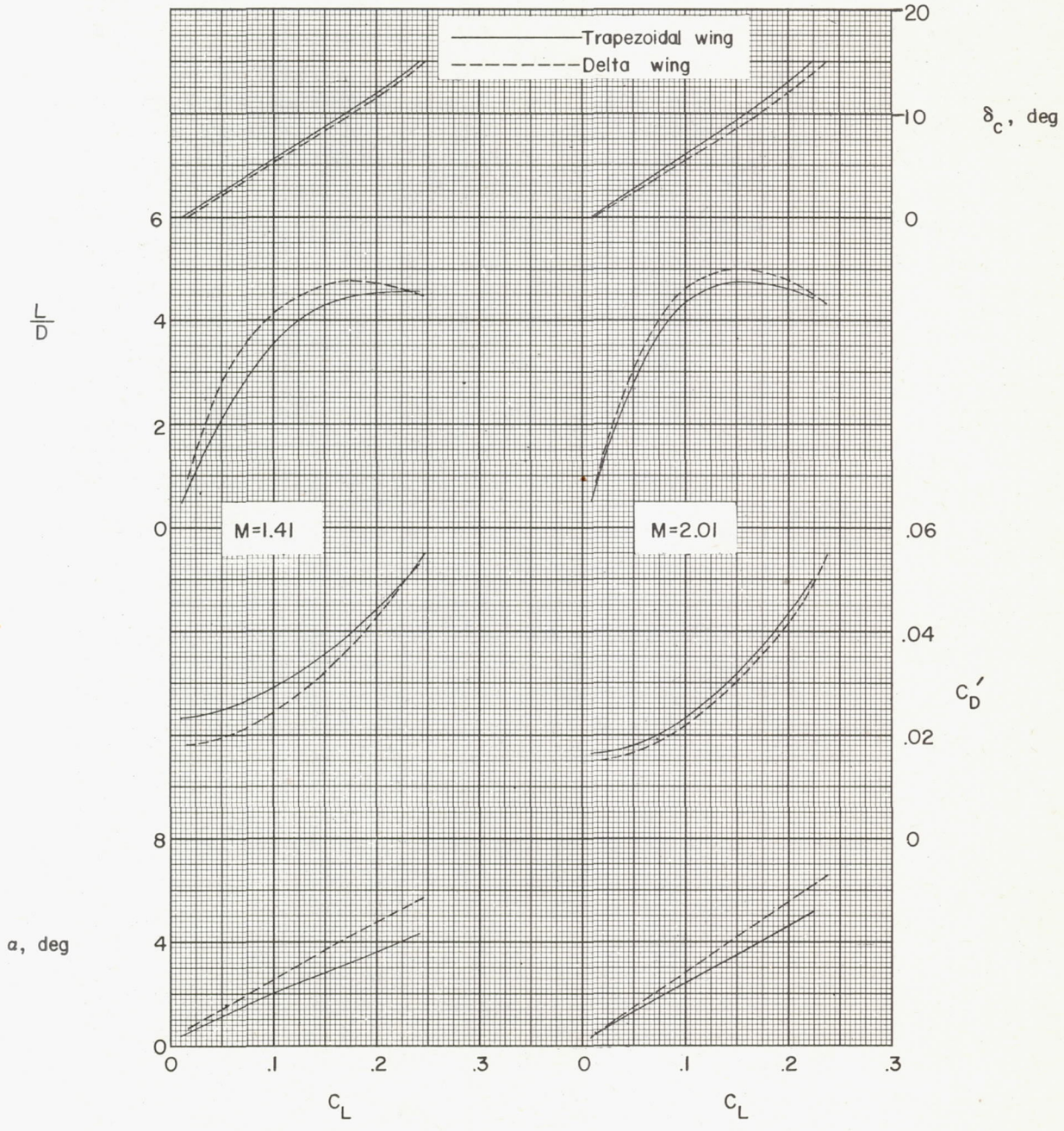


Figure 12.- Trim longitudinal characteristics with center of gravity at body station 25.

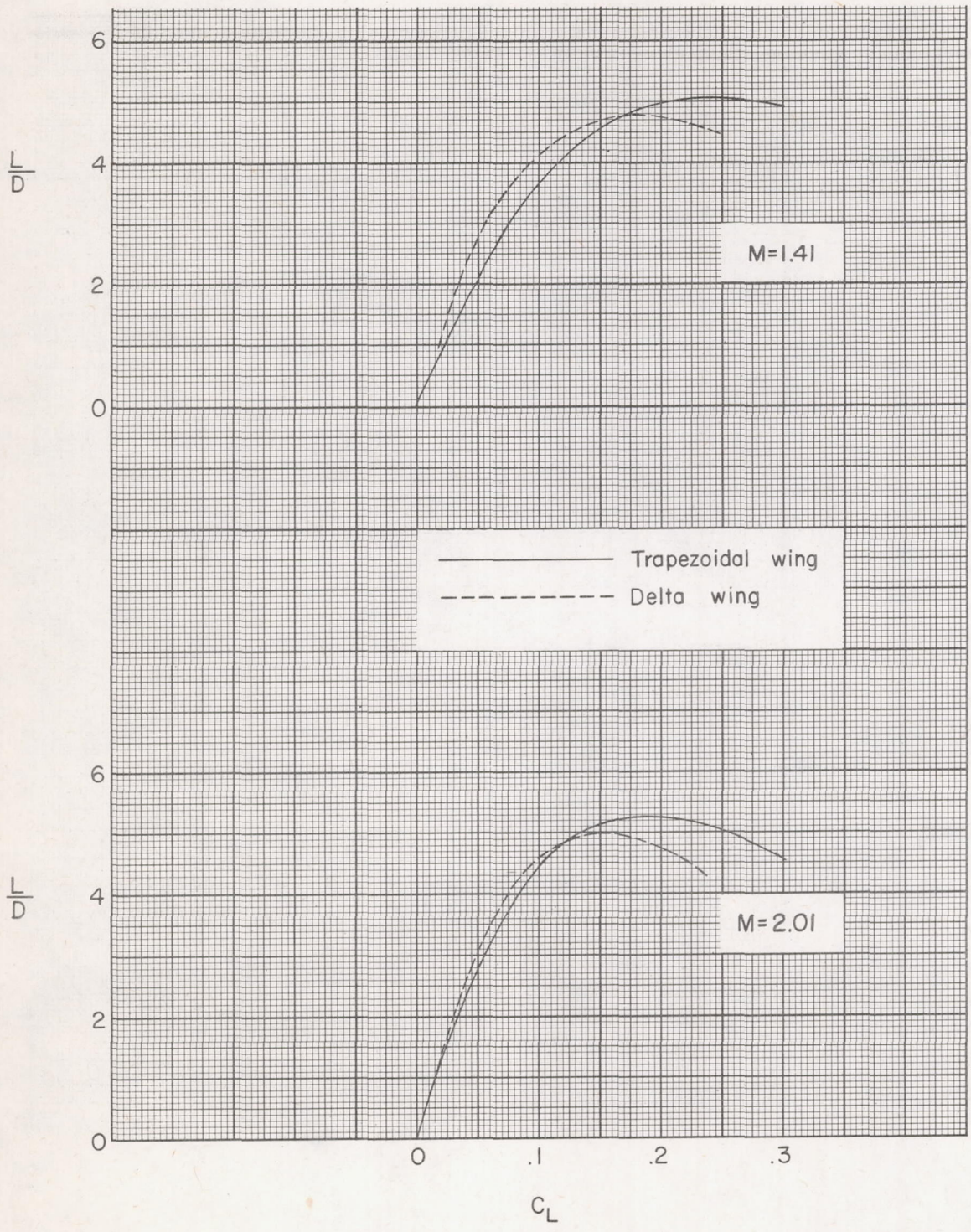


Figure 13.- Trim L/D characteristics with equal static margins ($0.22\bar{c}$).

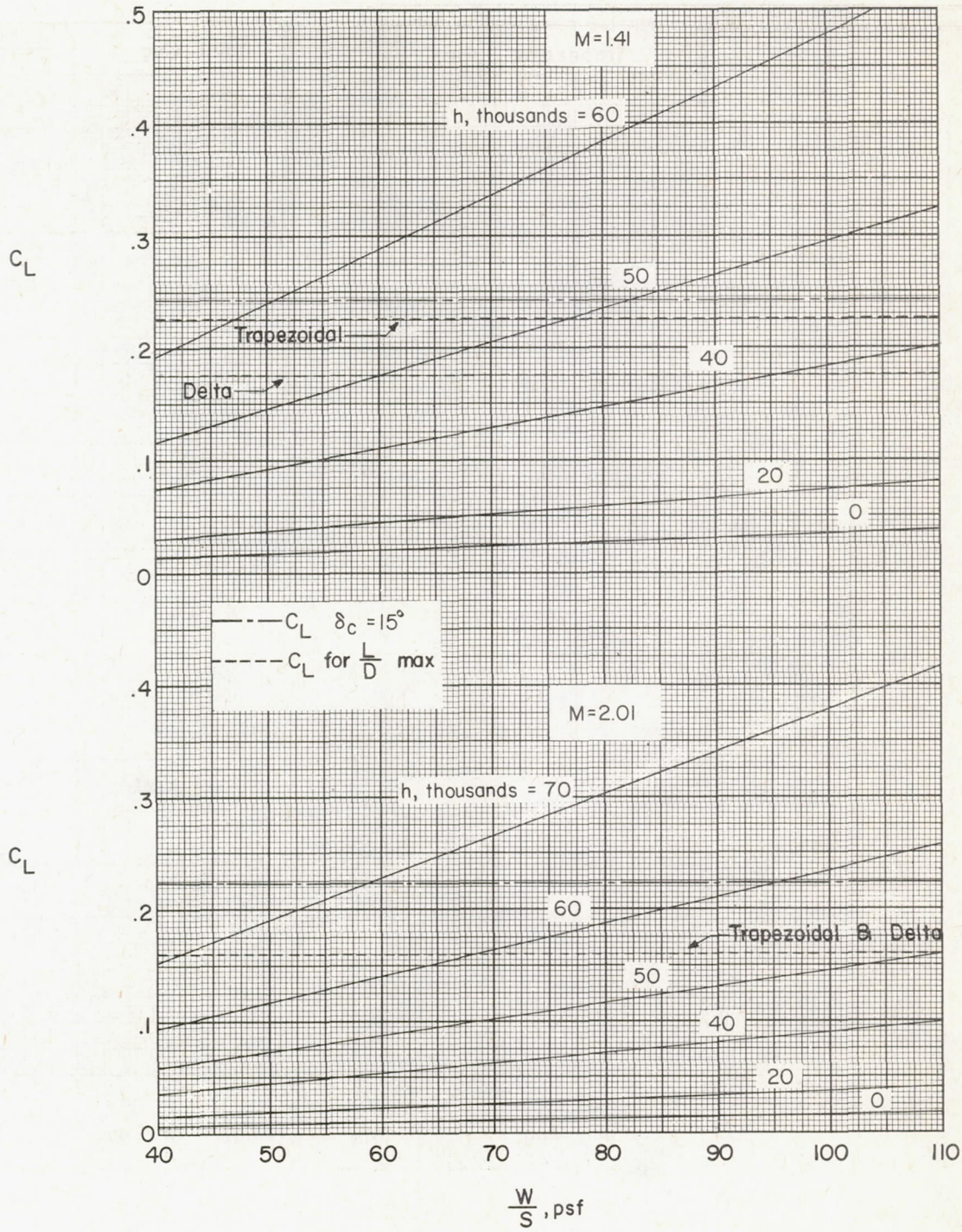
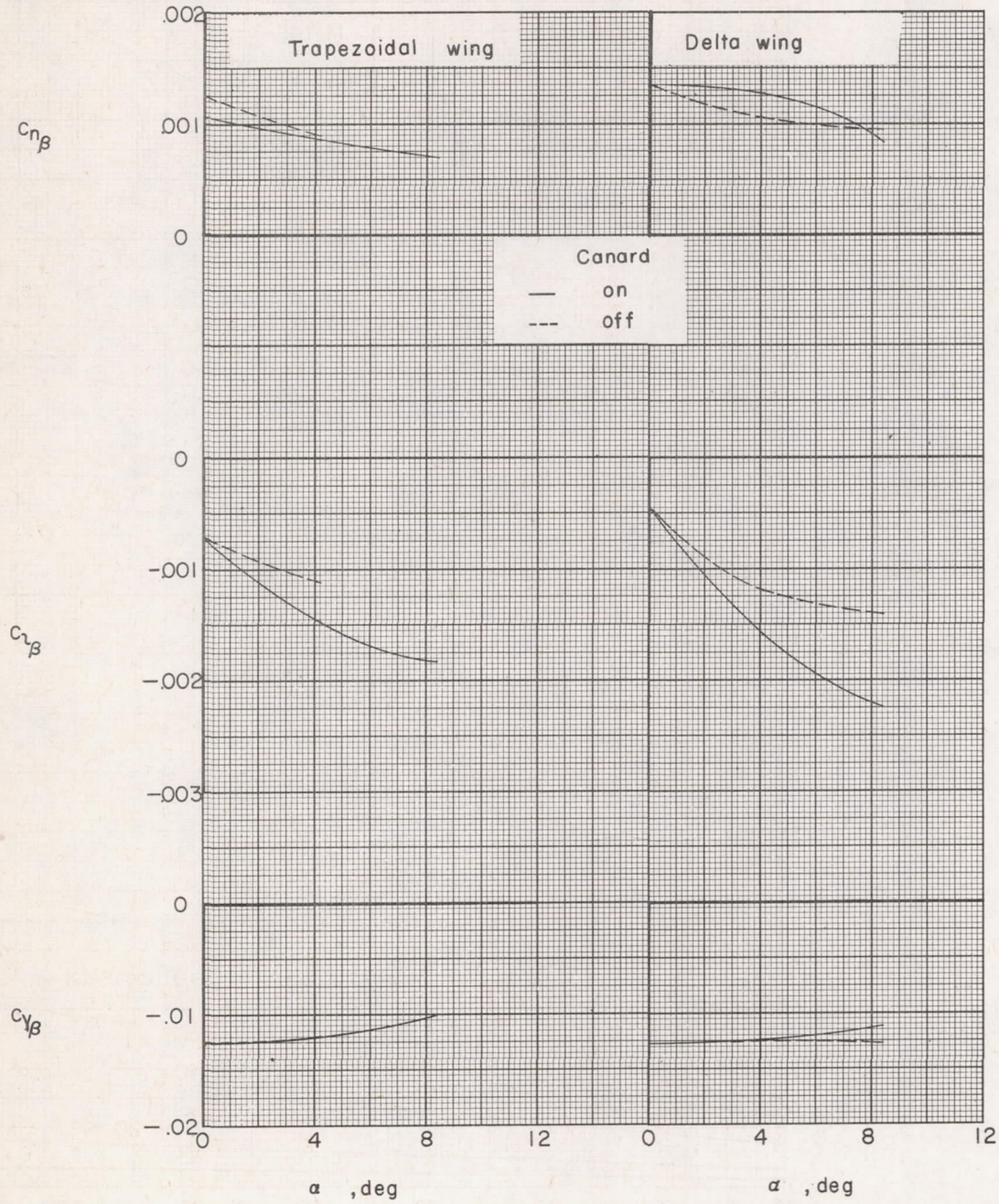
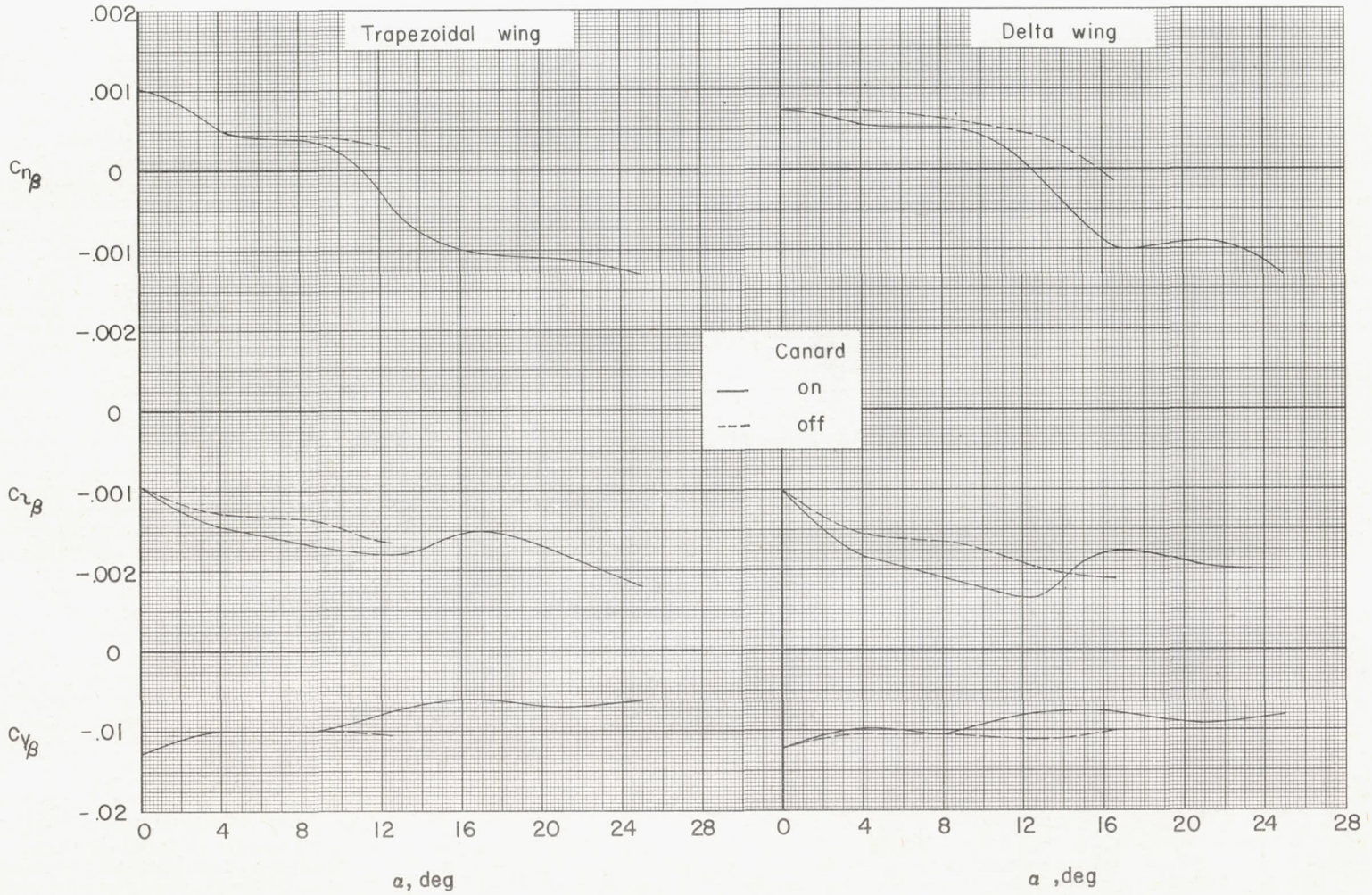


Figure 14.- Variation with wing loading and altitude of the lift coefficient required for level flight.



(a) M = 1.41.

Figure 15.- Variation of sideslip derivitives with angle of attack for models with canard on and off.



(b) M = 2.01.

Figure 15.- Concluded.

NACA - Langley Field, Va.